Annu. Rev. Earth Planet. Sci. 2021.49:9-36. Downloaded from www.annualreviews.org
Access provided by University of Texas - Dallas on 06/01/21. For personal use only.

ANNUAL REVIEWS

Annual Review of Earth and Planetary Sciences

The Geodynamic Evolution of Iran

Robert J. Stern,[1] Hadi Shafaii Moghadam,[2] Mortaza Pirouz,[1] and Walter Mooney[3]

[1]Department of Geosciences, University of Texas at Dallas, Richardson, Texas 75080, USA; email: rjstern@utdallas.edu

[2]School of Earth Sciences, Damghan University, Damghan 36716-41167, Iran

[3]Earthquake Science Center, US Geological Survey, Menlo Park, California 94025, USA

Annu. Rev. Earth Planet. Sci. 2021. 49:9–36

The *Annual Review of Earth and Planetary Sciences* is online at earth.annualreviews.org

https://doi.org/10.1146/annurev-earth-071620-052109

Copyright © 2021 by Annual Reviews.
All rights reserved

ANNUAL REVIEWS CONNECT

www.annualreviews.org

- Download figures
- Navigate cited references
- Keyword search
- Explore related articles
- Share via email or social media

Keywords

plate tectonics, continental collision, subduction initiation, ophiolite, magmatic arc, earthquake

Abstract

Iran is a remarkable geoscientific laboratory where the full range of processes that form and modify the continental crust can be studied. Iran's crustal nucleus formed as a magmatic arc above an S-dipping subduction zone on the northern margin of Gondwana 600–500 Ma. This nucleus rifted and drifted north to be accreted to SW Eurasia ~250 Ma. A new, N-dipping subduction zone formed ~100 Ma along ~3,000 km of the SW Eurasian margin, including Iran's southern flank; this is when most of Iran's many ophiolites formed. Iran evolved as an extensional continental arc in Paleogene time (66–23 Ma) and began colliding with Arabia ~25 Ma. Today, Iran is an example of a convergent plate margin in the early stages of continent-continent collision, with a waning magmatic arc behind (north of) a large and growing accretionary prism, the Zagros Fold-and-Thrust Belt. Iran's crustal evolution resulted in both significant economic resources and earthquake hazards.

- Iran is a natural laboratory for studying how convergent plate margins form, evolve, and behave during the early stages of continental collision.
- Iran formed in the past 600 million years, originating on the northern flank of Gondwana, rifting away, and accreting to SW Eurasia.

- Iran is actively deforming as a result of collision with the Arabian plate, but earthquakes do not outline the position of the subducting slab.
- The Cenozoic evolution of Iran preserves the main elements of a convergent plate margin, including foredeep (trench), accretionary prism, and magmatic arc.

1. INTRODUCTION

Iran is home to one of the world's oldest civilizations, with urban settlements dating back to 7000 BC. This long-lived culture was fostered by Iran's geology, which created a region conducive to agriculture and trade that was not easily invaded. In this review, we discuss the geodynamic evolution of Iran that produced the landscape on which these civilizations thrived. Iran encompasses a large area (~1.65 million km^2), more than 4 times the size of Japan, about 2.5 times the size of France, and more than twice the size of Texas (**Figure 1**). It is nestled between three seas: the Caspian on the north, the Persian Gulf on the south, and the Gulf of Oman on the southeast. It is also framed by two great mountain chains: the Zagros Mountains, a series of parallel ridges along its southwestern margin, and the rugged Alborz Mountains along its northern margin (**Figure 1**). The Alborz Mountains have Iran's highest peaks including Mount Damavand (5.6 km above sea level) (**Figure 1**), which is also the tallest volcano in Asia. Many Zagros peaks are taller than 3 km above sea level, and five are higher than 4 km. NW Iran is a part of the Armenian Highlands, the southern continuation of the Caucasus Mountains. Behind these seas and mountains, the interior of Iran comprises several closed basins within the Central Plateau, which mostly lies ~1 km above sea level. The eastern Iranian Plateau is arid and includes two salt deserts, the Dasht-e Kavir and the Dasht-e Lut (**Figure 1**). The rugged mountains of Afghanistan mark Iran's natural eastern boundary.

Earth's continental crust can be subdivided into six distinct types based on geologic considerations: shield, platform, orogen, basin, large igneous province, and extended crust (Mooney 2015). The crust of Iran is best classified as orogen, defined by the US Geological Survey (USGS) as "a linear or arcuate region that has been subjected to folding and other deformation during an orogenic cycle" (Neuendorf et al. 2011, p. 457). Bird (2003) also describes Iran as an orogen, which is defined as a complex region with areas of distributed deformation and uplift. Although Iran is indeed an orogen, this classification does not adequately describe this unique geologic province, which motivates this overview.

Iran's distinctive geodynamic setting provides a unique opportunity to study crust formation, terrane accretion, subduction initiation, continental collision, and the evolution of a continental convergent margin and its transition into a continental collision zone. From a global perspective, orogens span a range of complexity, from the simplicity of Cuba, which represents single subduction initiation, collisional, and strike-slip faulting events, to the complexity of the Central Asian Orogenic Belt, which was formed by multiple tectonic episodes. Intermediate in complexity, the Iran orogen preserves a 600-million-year history of diverse plate tectonic processes, reflecting a remarkable odyssey. Its nucleus began as part of an enormous continental magmatic arc that extended 5,000 km along the northern margin of the Ediacaran supercontinent Greater Gondwana or Pannotia. A backarc basin opened, separating the arc from the supercontinent and allowing the nucleus to drift northward across the Paleotethys Ocean to collide with Eurasia. Thus accreted to Eurasia, Iran then developed a passive continental margin on its southern margin that transformed with time into a convergent margin. The modern tectonic environment was created when

Annu. Rev. Earth Planet. Sci. 2021.49:9-36. Downloaded from www.annualreviews.org
Access provided by University of Texas - Dallas on 06/01/21. For personal use only.

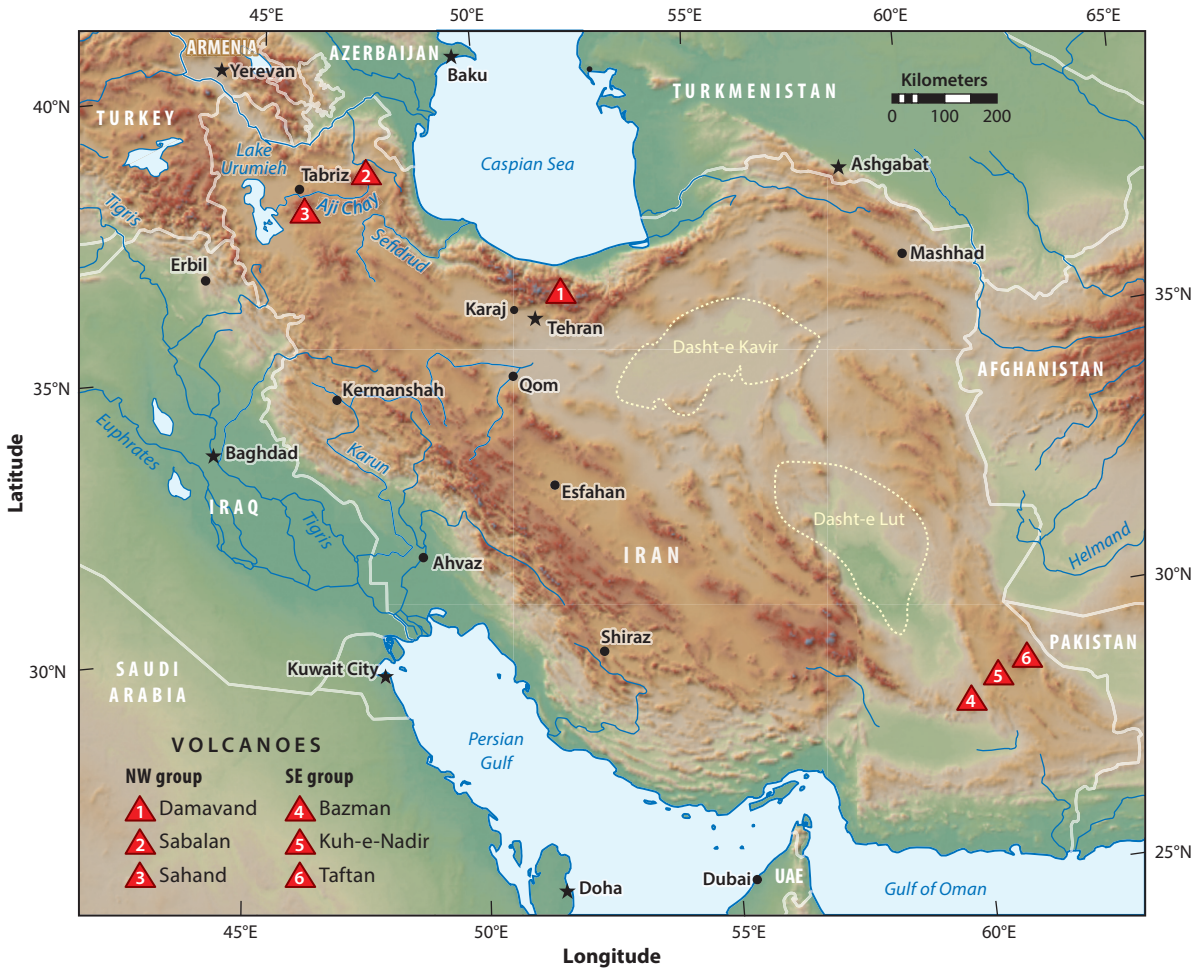

Figure 1

Topographic map of Iran showing major rivers, lakes, deserts, volcanoes, and cities with populations greater than 1,000,000. Abbreviation: UAE, United Arab Emirates.

the Arabian plate rifted away from NE Africa, drifted north, and started colliding with Iran, which it continues to do today (Stampfli & Borel 2002).

Most of Iran's continental crust formed during a burst of igneous activity in the Ediacaran and early Cambrian around 600 to 500 Ma during what is known in western Europe as the Cadomian orogeny (Garfunkel 2015). The proto-crust of Iran, in addition to that of Turkey and other Cadomian tracts to the west, formed as a broad magmatic arc along the northern margin of Gondwana. This embryonic arc (along with Anatolia) rifted from Gondwana during the late Paleozoic as part of the ribbon continent Cimmeria. The northward migration of Cimmeria terminated as it collided with Eurasia and closed the Paleozoic Paleotethys seaway. This collision created the Permian–Triassic suture along Iran-Anatolia's northern margin. Prior to this collision and for some time afterward, southern Iran-Anatolia served as a passive margin on the northern margin of Neotethys (Stampfli 2000, Stampfli et al. 2001). Jurassic–Early Cretaceous rifting weakened the lithosphere along the SW margin of Iran. This weakness collapsed in the Late

Annu. Rev. Earth Planet. Sci. 2021.49:9-36. Downloaded from www.annualreviews.org
Access provided by University of Texas - Dallas on 06/01/21. For personal use only.

Cretaceous to form an N-dipping subduction zone on the southern edge of Iran. Subduction initiation generated a forearc ophiolite belt that stretched 3,000 km from Cyprus to Oman, and strong extension also affected Iran crust as far north as the Caspian Sea. As sediments were scraped off the subducting plate, the Zagros Fold-and-Thrust Belt began to grow against this ophiolitic forearc backstop. The Zagros Fold-and-Thrust Belt is thus an accretionary wedge in the Iranian forearc that continues to grow as northern Arabia collides with Iran's southern margin.

In this overview, we review the current understanding of the crust and upper mantle beneath Iran. We first summarize what is known about Iran's modern plate tectonic setting before outlining Iran's geotectonic domains, each of which contains useful information about how Iran evolved. We finish by highlighting some opportunities for future research. This overview is not exhaustive, but it is inclusive. The hope is that it will provide a useful foundation for future research on this important orogen.

Annu. Rev. Earth Planet. Sci. 2021.49:9-36. Downloaded from www.annualreviews.org
Access provided by University of Texas - Dallas on 06/01/21. For personal use only.

2. CENOZOIC PLATE TECTONIC SETTING

The northern and central parts of modern Iran collided with and were accreted to the Eurasian plate in the Permian–Triassic (~250 Ma), and now Arabia is colliding with Iran. The Arabian plate is one of the youngest plates on Earth, originating only ~25 Ma via rifting of NE Africa along the Gulf of Aden and the Red Sea (Stern & Johnson 2010). How long N-dipping subduction beneath Iran has been going on is highly debated, with estimates ranging from since about 200 Ma (Stampfli & Borel 2002) to 100 Ma (Shafaii Moghadam & Stern 2011). The Zagros Fold-and-Thrust Belt is a result of northward subduction beneath Iran and grew in two main stages: (*a*) subduction of Neotethys and the African plate (before about 25 Ma) and (*b*) Eurasia-Arabia collision (about 25 Ma–present) (Pirouz et al. 2017). Convergence was accompanied by Late Cretaceous and Cenozoic igneous activity; these subduction-related partial melts and fluids have contributed to the thermal weakening of the Iranian lithosphere over the past 100 Ma, facilitating deformation.

Lithosphere beneath eastern Arabia and the Zagros (**Figure 2*b***) is thick (up to 210 km thick) (Jiménez-Munt et al. 2012) and strong, whereas that beneath Iran north of the Zagros is thin. The Iranian Plateau is underlain by lithosphere that is 130 to 160 km thick. Lithosphere is thinnest and weakest beneath the Lut and Jaz Murian basins where it is estimated to be ~125 and ~135 km thick, respectively (Jiménez-Munt et al. 2012). Consequently, Arabia behaves as a strong rigid plate and can be described by the "plate tectonic approximation" (Gordon 1998) whereby motions anywhere on the plate can be assessed with a pole of rotation and an angular velocity (the Euler pole for Arabia lies at about 50°N, 10°W, and rotation is about 0.5°/Ma) (Alothman et al. 2016). In contrast, the weak lithosphere of Iran deforms internally and is best described as a "diffuse plate boundary" (Gordon 1998). **Figure 3** uses the GPS-derived velocity field to show how Iran and surrounding regions deform (Reilinger & McClusky 2011). These differences in deformation behavior are directly related to the thickness (**Figure 2*b***) and strength of the two lithospheres. For example, the Arabia-Eurasia collision zone is marked by a striking change in lithospheric thickness, with the thickest lithosphere beneath the Mesopotamian foreland basin and the thinnest lithosphere beneath the Iranian Plateau and the Zagros Mountains.

Crust thickness also varies across Iran (**Figure 2*a***). Whereas stable continental crust has an average thickness of 40 km (Christensen & Mooney 1995), the crust of Iran is 40–60 km thick. Thickened crust is expected for an orogen, in comparison with the 40-km average thickness of stable continental crust. The NNW-SSE-trending zone of 50–60-km-thick crust mostly underlies the Iranian Plateau. The thinnest crust (30–35 km) is found in two locations: beneath the southern Caspian Sea and near the border with Pakistan in southeastern Iran (**Figure 2*a***). The southern

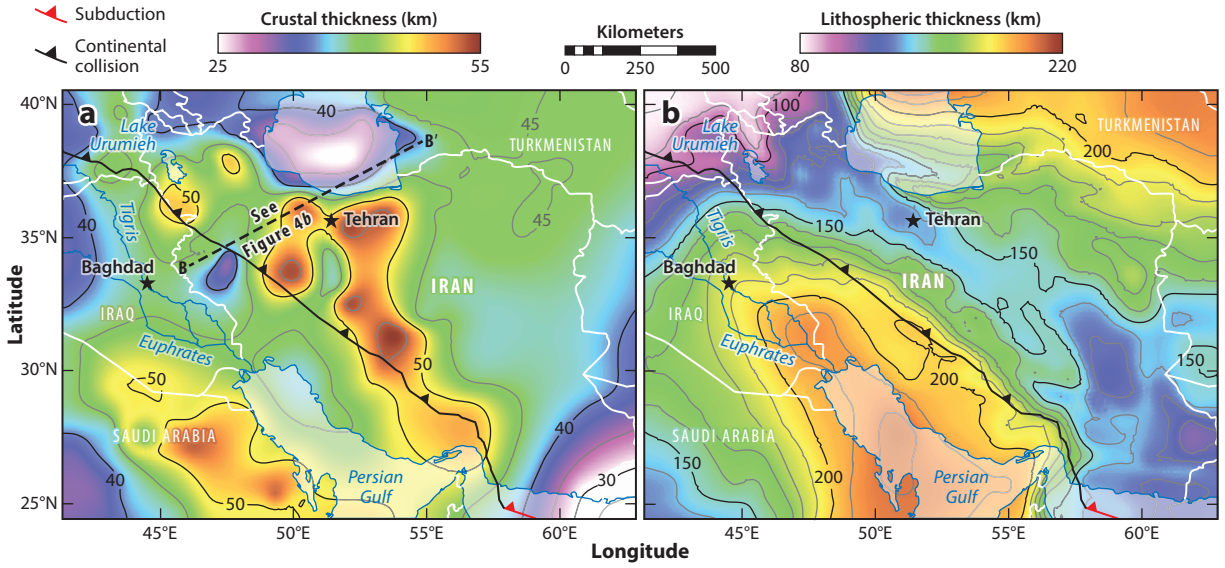

Figure 2

Crust and lithosphere thicknesses for Iran and surrounding regions. (*a*) Crustal thickness for Iran and neighboring regions based on seismic measurements. We estimate uncertainties in crustal thickness to be 20%, which is +/−8 km for 40-km-thick crust. Data from Prodehl & Mooney (2012) and Mooney (2015). The thick dashed black line shows the location of the tomographic section in **Figure 4**. (*b*) Lithospheric thickness determined by combining topography and the geoid beneath Arabia and Iran (Jiménez-Munt et al. 2012).

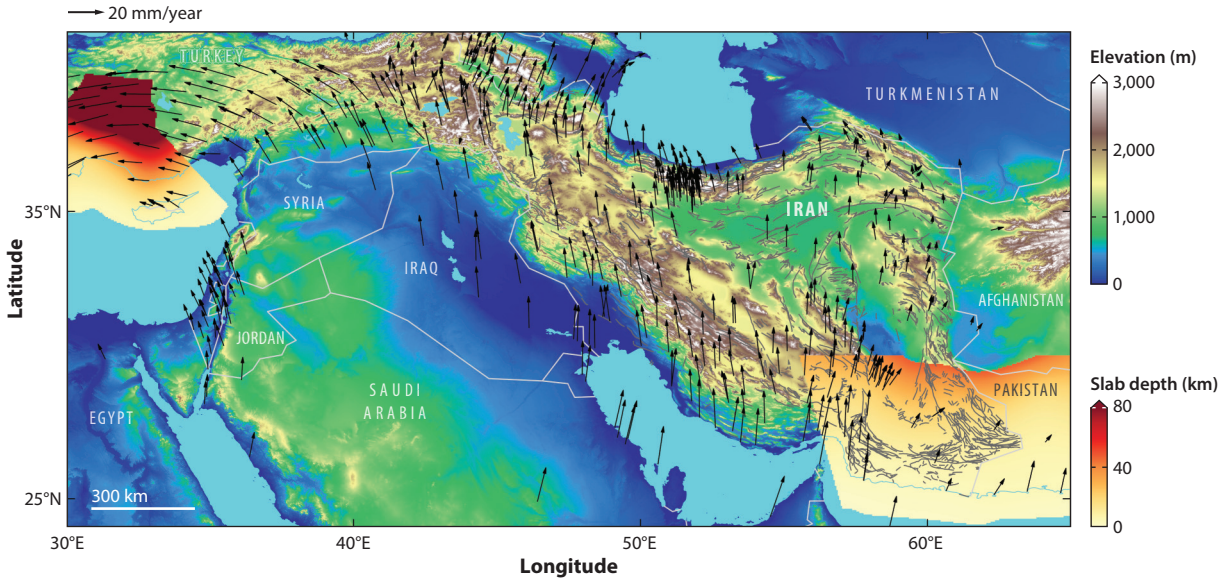

Figure 3

Neotectonic setting of Iran showing deformation of Iran and surrounding regions. Note regions that are underlain by subducted lithosphere of the African plate in the west and Arabian plate in the east (*yellow-orange* regions) and the intervening ~2,500 km where no subducting slab is imaged. Arrows are GPS velocities determined for Africa, Arabia, and Iran with respect to Eurasia. GPS data from Khorrami et al. (2019) and Blewitt et al. (2018). Sites used to construct the Eurasia plate model from supplementary table S2 of Altamimi et al. (2017). Geometry of subducted slab from Hayes et al. (2018). Elevation data from Jarvis et al. (2008).

Annu. Rev. Earth Planet. Sci. 2021.49:9-36. Downloaded from www.annualreviews.org
Access provided by University of Texas - Dallas on 06/01/21. For personal use only.

Caspian Sea has been explored extensively for oil and gas using seismic methods. These studies reveal 15 to 20 km of sediments that are underlain by thin (15–20 km), high-density crust that may be a trapped piece of thickened oceanic crust or highly extended continental crust (Jackson et al. 2002). Just south of the Caspian Sea, the Alborz Mountains are underlain by 40–50-km-thick crust, whereas crust that is 50–60 km thick underlies central Iran. The thickest crust trends NNW-SSE across central Iran oblique to the NW-SE trend of the Zagros Mountains. This implies that crustal thickening may predate the modern Arabia-Eurasian collision.

The modern Iran landscape was largely shaped by an N-dipping subduction zone. Despite extensive studies in this region, it is unclear whether Iran is still underlain by an active subduction zone or if the subducted slab has broken off. As seen in **Figure 3**, Hayes et al. (2018) do not show a subducted slab for 2,000 km between the Makran and the eastern Mediterranean. We know that a subducted slab lies beneath the Makran region of SE Iran and also underlies SW Pakistan west of the Chamran left-lateral transform fault. Earthquakes extend to as deep as ∼120 km in the western Makran subduction zone (Nemati 2019) but are imaged much deeper by seismic tomography. The west edge of the Makran subduction zone lies beneath the N-S-trending Minab-Zendan right-lateral strike-slip fault, and this fault may lie above a slab tear or the western edge of the Makran slab. It is unknown whether there is a continuous subducted slab west of the Minab-Zendan fault or if the subducted slab has broken off.

Many researchers argue for slab breakoff beneath Iran (e.g., Agard et al. 2011, Garzanti et al. 2018). Arguments for this include a lack of deep seismicity west of the Makran subduction zone (Zare et al. 2014). However, some active subduction zones do not experience deep earthquakes, such as Cascadia along the NW North American margin. Perhaps salt and oil on top of the sinking Arabian plate lubricate the plate interface, allowing more aseismic slip and few earthquakes? We know that Arabia has continued its northward motion uninterrupted for most of Cenozoic time (McQuarrie et al. 2003), so something must still be pulling it. Seismic tomography is useful for addressing the question of whether a subducted slab lies beneath Iran today. Mahmoodabadi et al. (2019) investigated the upper mantle structure beneath Iran using a dense array of seismometers. As is evident in their P-wave cross section (**Figure 4*a***), the upper mantle beneath Iran is characterized by pronounced (±8%) zones of high and low seismic velocities. A high-velocity body at a depth of 40 to 200 km is visible beneath the Zagros Mountains and corresponds to the subducting Arabian plate, as previously suggested by Alinaghi et al. (2007). Detached high-velocity bodies centered at 325 km and 425 km may be subducted Tethyan oceanic lithosphere, as also evidenced in gravity inversions (Kaban et al. 2016). There is a pronounced low seismic velocity immediately below the Moho beneath the Sanandaj-Sirjan Zone, Urumieh-Dokhtar magmatic belt, and central Iran. The high topography of these regions can be attributed to the buoyancy forces of this low-velocity, low-density zone in the uppermost mantle. The seismic tomography cross section (**Figure 4**) also suggests the presence of a westward-dipping subduction zone beneath the Alborz Mountains, although the strength of this anomaly is less than the clearer anomaly beneath the Zagros Mountains.

There are other lines of evidence that bear on the question of whether there is a subducted slab beneath Iran today. The Red Sea continues to open, with active seafloor spreading inferred for at least the southern half (Stern & Johnson 2019), and slab pull is required to drive this process. The Mesopotamian–Persian Gulf foredeep suggests that something is pulling the Arabian plate down. Furthermore, magmatic activity along the Urumieh-Dokhtar magmatic belt and other Cenozoic magmatic belts of Iran is waning. Is Urumieh-Dokhtar magmatic belt magmatism decreasing due to slab breakoff and/or delamination, or does it reflect the fact that continental crust and sediments are now being subducted instead of Neotethyan oceanic lithosphere? Clearly, additional geologic observations and geophysical experiments that focus on identifying the subducted slab

Annu. Rev. Earth Planet. Sci. 2021.49:9-36. Downloaded from www.annualreviews.org
Access provided by University of Texas - Dallas on 06/01/21. For personal use only.

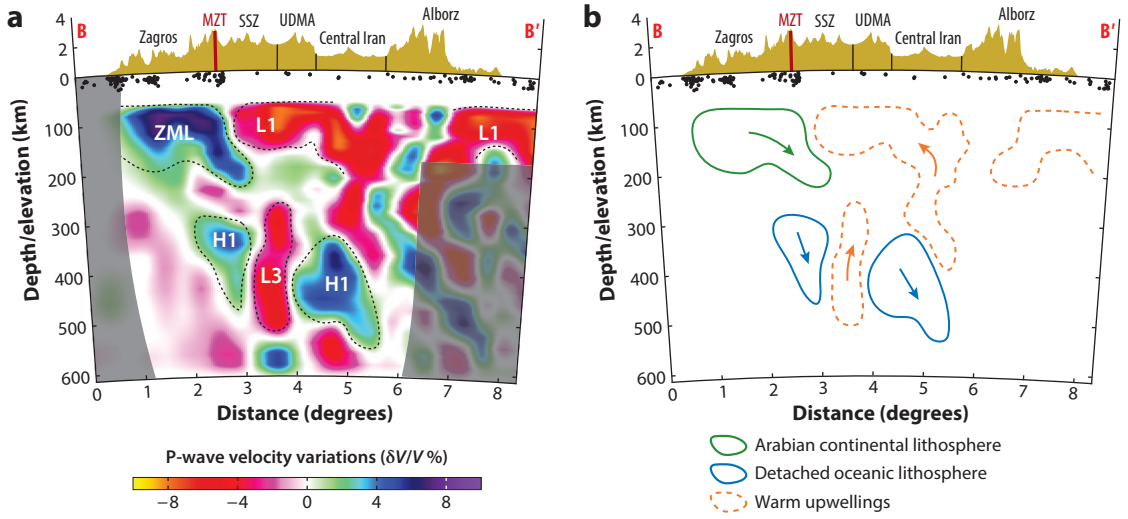

Figure 4

(*a*) P-wave seismic tomography cross sections across northern Iran from Iraq to the Alborz Mountains (Mahmoodabadi et al. 2019). The location is shown on **Figure 2**. Topography is indicated in light brown. (*b*) Interpretation of seismic tomography cross section. Subduction of the Zagros Mountains can be imaged to a depth of 200 km. Deeper high-seismic-velocity bodies, outlined with solid lines, may be detached slabs of oceanic lithosphere. Sinking dense material is compensated by upwelling warm mantle material with a low seismic velocity, outlined with dashed lines. Abbreviations: H1, mantle high-velocity zones; L1 and L3, mantle low-velocity zones 1 and 3; MZT, Main Zagros Thrust; SSZ, Sanandaj-Sirjan Zone; UDMA, Urumieh-Dokhtar magmatic arc; ZML, Zagros mantle lithosphere.

and associated slab windows and broken-off slab fragments are needed to understand whether a continuous slab of subducted Arabian lithosphere underlies Iran today.

3. GEOTECTONIC DOMAINS OF IRAN

Iran evolved in six stages that produced distinct crustal units and fabrics. These elements are distributed between four megastructural zones in the form of three orogens surrounding a central stable block: (*a*) in the southwest adjacent to the convergent margin, the active NW-trending Zagros orogen, which consists of three forearc elements, from northeast to southwest: the Late Cretaceous forearc ophiolite belt (**Figure 5*d***), the Jurassic Sanandaj-Sirjan Zone (Azizi & Stern 2019, Hunziker et al. 2015) (**Figure 5*c***), and the Zagros Fold-and-Thrust Belt (**Figure 5*c***); (*b*) in the north, the Alborz orogen (**Figure 5*b***) with E-W-trending Paleozoic suture and modern deformation belt; (*c*) in the east, a broad N-S-trending deformation belt (**Figure 5*d***); and (*d*) in the middle, the Cadomian core intruded by Cenozoic igneous rocks (**Figure 5*a*,*e***). The four megastructural zones outlined above are reflected in the distribution of active faults where frequent and high-magnitude earthquakes occur (**Figure 6**). For example, many earthquakes, including two of the ten deadliest earthquakes since 1930 (**Table 1**), occurred on NW-trending faults that run through the Zagros region (**Figures 5*d*** and **6**). Four of the ten deadliest earthquakes since 1930 occurred near the Paleozoic suture zone in the north, while the remaining four occurred along the N-S deformation belt in the east. The central Cadomian core, however, is seismically quiet.

The distribution of active faults and earthquakes reflects Iran's geologic evolution. The record of this evolution is preserved in three main spatiotemporal realms of Iran: (*a*) older Iran crust

Annu. Rev. Earth Planet. Sci. 2021.49:9-36. Downloaded from www.annualreviews.org
Access provided by University of Texas - Dallas on 06/01/21. For personal use only.

Annu. Rev. Earth Planet. Sci. 2021.49:9-36. Downloaded from www.annualreviews.org
Access provided by University of Texas - Dallas on 06/01/21. For personal use only.

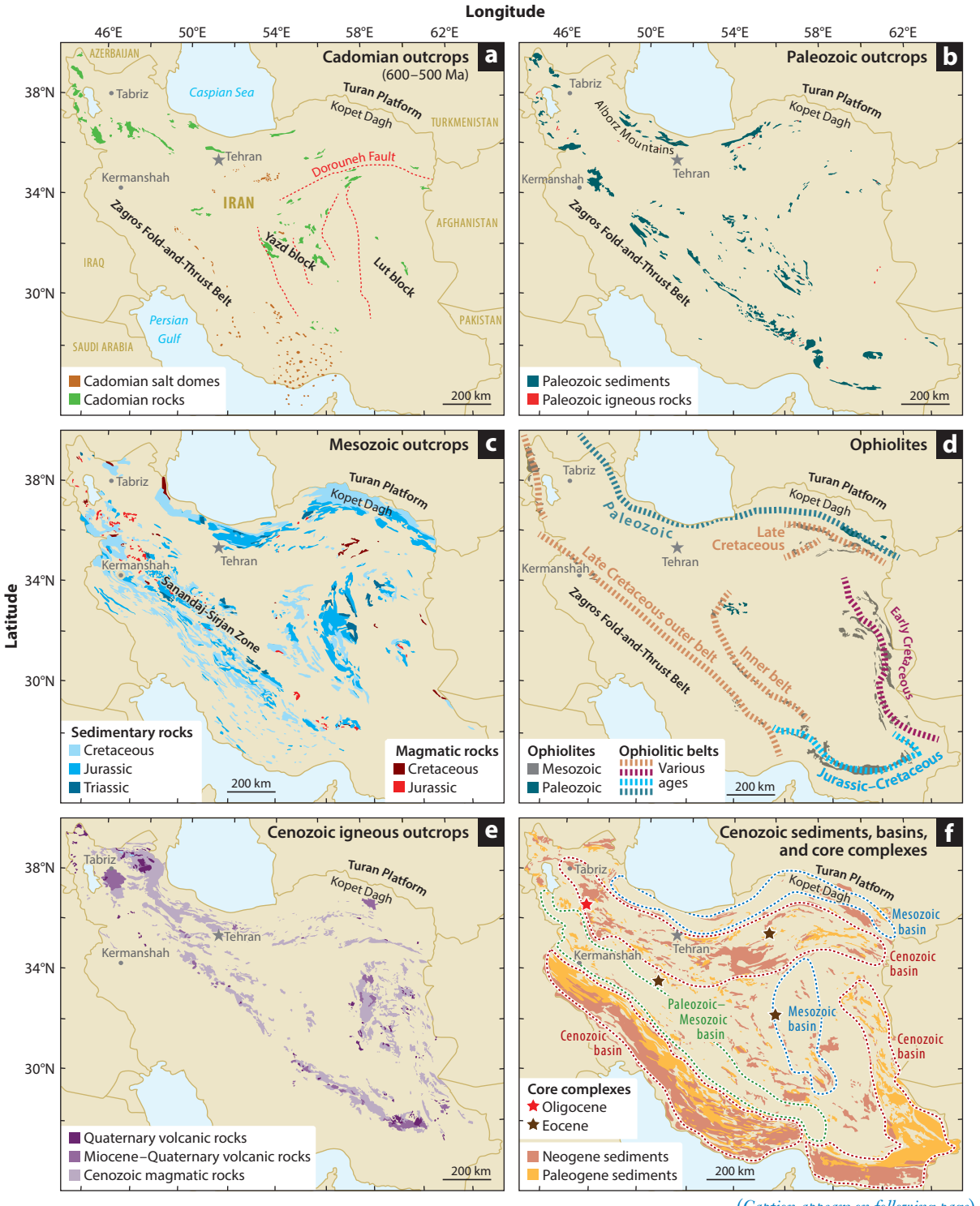

(*Caption appears on following page*)

Figure 5 (*Figure appears on preceding page*)

Geology time slices of Iran outcrops: (*a*) Cadomian rocks, including igneous, metamorphic, sedimentary, and evaporite rocks; (*b*) Paleozoic sedimentary and igneous rocks; (*c*) Early Cretaceous and Jurassic igneous and sedimentary rocks; (*d*) Paleozoic, Jurassic, and Cretaceous ophiolites; (*e*) Cenozoic igneous rocks; (*f*) Cenozoic sediments and locations of sedimentary basins. Eocene and Oligocene metamorphic core complexes are also shown.

and sediments, (*b*) younger (Late Cretaceous–Cenozoic) crust and sediments, and (*c*) the Zagros Fold-and-Thrust Belt. Older and younger crusts and sediments are separated by the Iranian tectonic revolution, which occurred in Late Cretaceous time when subduction initiated on the southern flank of Iran and northward subduction began. The Zagros Fold-and-Thrust Belt is treated separately because it continues to grow by accretion, is underlain by subducted Arabian crust, and is composed of Paleozoic, Mesozoic, and Cenozoic sediments. The Main Zagros Thrust (**Figures 6** and **7**) separates the Zagros Fold-and-Thrust Belt from crystalline crust of Iran. These three main spatiotemporal realms of Iran are outlined further below.

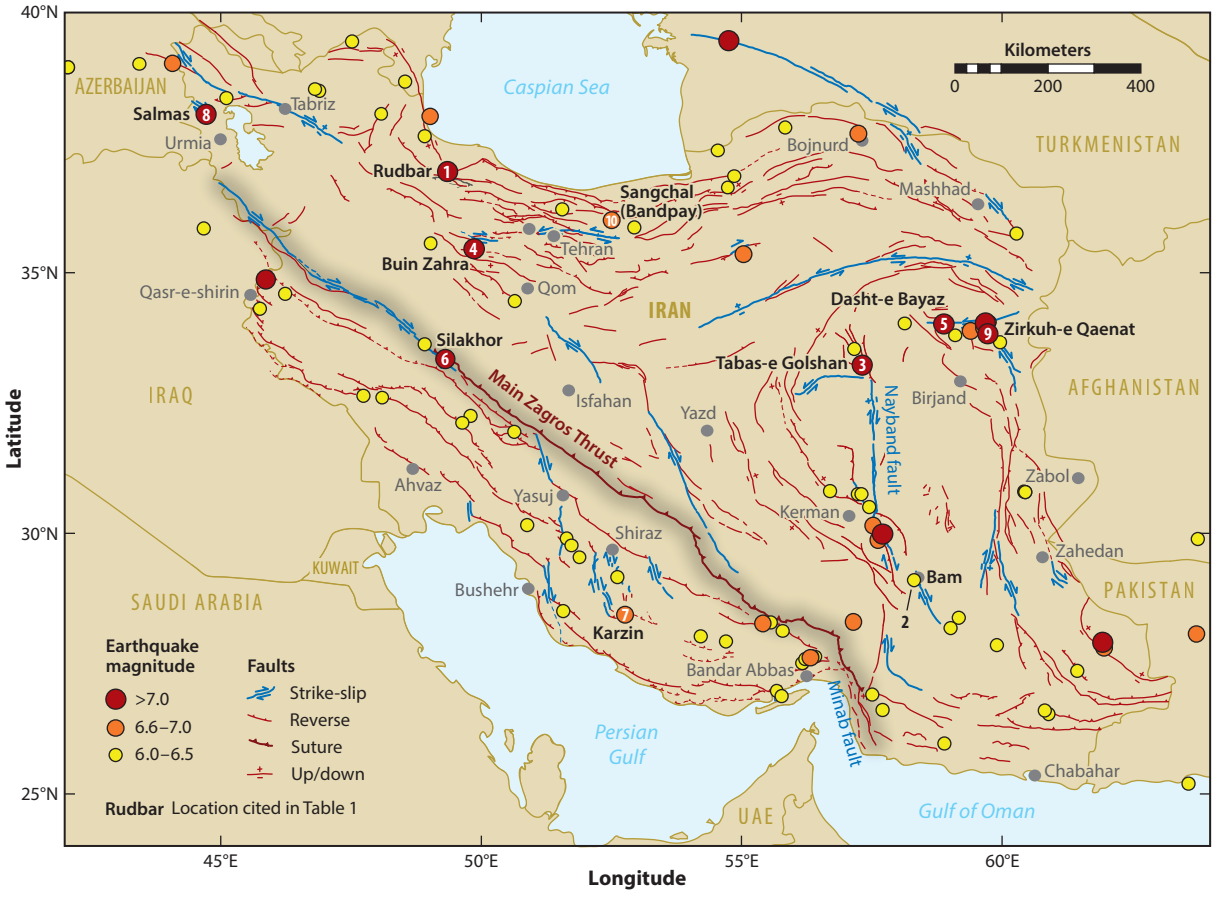

Figure 6

Active fault map and 1900–2019 epicenters of large earthquakes (>6.0 magnitude) in Iran. Numbers on the map correspond to the deadliest 10 earthquakes from 1909 to 2003 reported in **Table 1**. Abbreviation: UAE, United Arab Emirates. Figure adapted from Berberian (2014) and Hessami et al. (2003).

Annu. Rev. Earth Planet. Sci. 2021.49:9-36. Downloaded from www.annualreviews.org
Access provided by University of Texas - Dallas on 06/01/21. For personal use only.

Table 1 Instrumental records of the 10 deadliest earthquakes in Iran

Number	Date	Epicenter (°latitude North–°longitude East)	Location	M_b	M_s	M_w	Fault type	Deaths
1	June 20, 1990	36.99–49.22	Rudbar	6.2	7.4	7.3	Reverse fault with left lateral strike-slip component	40,000
2	December 26, 2003	28.95–58.27	Bam	5.9	6.6	6.6	Right lateral strike-slip fault	37,500
3	September 16, 1978	33.24–57.38	Tabas-e Golshan	6.7	7.4	7.3	Reverse fault	20,000
4	September 2, 1962	35.55–49.83	Buin Zahra	6.9	7.2	7.2	Reverse fault	12,200
5	August 31, 1968	34.04–58.95	Dasht-e Bayaz	6.0	7.2	7.1	Left lateral strike-slip fault	10,000
6	January 23, 1909	33.38–49.28	Silakhor	7.2	7.4	7.4	Right lateral strike-slip fault	8,000
7	April 10, 1972	28.41–52.78	Karzin	6.0	6.9	7.6	Reverse fault	5,010
8	May 6, 1930	38.15–44.67	Salmas	7.0	7.2	7.1	Reverse fault with right lateral strike-slip component	2,514
9	May 10, 1997	33.84–59.81	Zirkuh-e-Qaenat	6.5	7.2	7.2	Right lateral strike-slip fault	1,568
10	July 2, 1957	36.06–52.48	Sangchal (Bandpay)	7.0	6.8	7.1	Reverse fault	1,500

Numbered locations shown in **Figure 6**. Abbreviations: M_b, body wave magnitude; M_s, surface wave magnitude; M_W, moment magnitude. Table modified from Berberian (2014).

Annu. Rev. Earth Planet. Sci. 2021.49:9-36. Downloaded from www.annualreviews.org
Access provided by University of Texas - Dallas on 06/01/21. For personal use only.

3.1. Older Iran Crust and Sediments

Four Iran crustal units are discussed below (**Figure 5*a–f***): (*a*) Cadomian basement, (*b*) Paleozoic rocks, (*c*) Sanandaj-Sirjan Zone, and (*d*) Mesozoic sedimentary rocks. These rocks are treated together because they formed before the Iranian tectonic revolution occurred in Late Cretaceous time.

3.1.1. Cadomian basement. Most Iranian crust formed as part of an ~5,000-km-long continental arc on the northern flank of the Greater Gondwana supercontinent during the Cadomian episode in late Ediacaran and early Cambrian time (600–500 Ma). Cadomian igneous and metamorphic rocks make up much of the crust of western and southern Europe. Cadomian crust can be traced eastward into SE Europe, Anatolia, and Iran and perhaps further into Central Asia. Cadomian rocks of Iran are very similar to those of Anatolia.

Outcrops of Neoproterozoic–Early Cambrian (Cadomian) rocks are widespread in Iran (e.g., Golpayegan, Khoy-Urumieh, Zanjan-Takab, Torud, Taknar, Saghand) (**Figure 5*a***) and also in Anatolia. These outcrops are mostly gneisses and granites ranging in age from 600 to 500 Ma (Shafaii Moghadam et al. 2017) but also include overlying Ediacaran metasediments. Cadomian gneiss and granitoids of Iran formed on the northern margin of Gondwana as a broad magmatic arc above an S-dipping subduction zone. Arc magmatism was especially intense during a magmatic flare-up from 570 to 525 Ma. Crust formation as a result of Cadomian arc magmatism in Iran and Turkey occurred at a rate of ~0.6 km^3/Ma, a significant fraction of the global arc crust production rate of 1.65 km^3/Ma (Reymer & Schubert 1984). There is abundant Hf and Nd isotopic evidence of ~1.8 Ga crust, but no pre-Cadomian rocks are known from either Iran or Turkey. One of the

Annu. Rev. Earth Planet. Sci. 2021.49:9-36. Downloaded from www.annualreviews.org
Access provided by University of Texas - Dallas on 06/01/21. For personal use only.

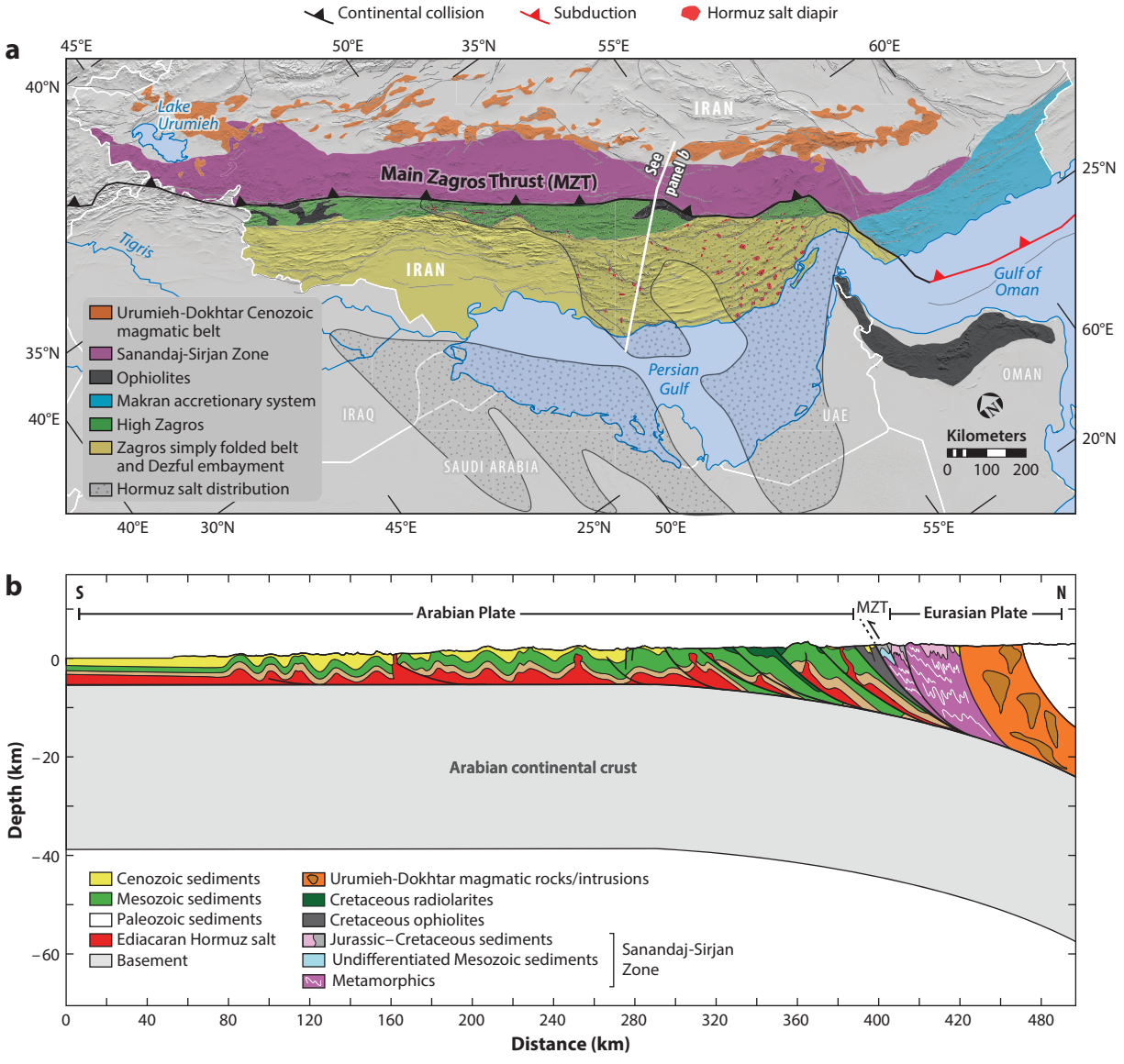

Figure 7

(*a*) Structural subdivisions along the edges of Arabia and Eurasia showing continental-continental collision zone changes to subduction toward the east in the Makran area. Panel adapted from Pirouz et al. (2017). (*b*) Crustal scale cross section across the Zagros Fold-and-Thrust Belt. Abbreviation: UAE, United Arab Emirates. Data from Huber (1976) and Pirouz et al. (2017).

many ways that Iran-Anatolia and Afghanistan differ is that pre-Ediacaran crust is documented for Afghanistan but not Iran-Anatolia, although zircon Hf and whole-rock Nd isotopic data for Iran-Anatolia igneous rocks point to widespread involvement of such older crust (Shafaii Moghadam et al. 2020a).

Cadomian arc crust exposed in Iran consists of a heterogeneous assemblage of magmatic rocks dominated by felsic plutons along with minor felsic extrusive rocks. Mafic magmatic rocks are less abundant. Three main varieties of Cadomian rocks are observed:

1. Calc-alkaline metagranites to metagabbros associated with mafic to felsic orthogneisses associated with subordinate mafic and felsic volcanic rocks. Paragneisses, metapsammites, and metapelites (metamorphosed in upper greenschist to upper amphibolite facies) with rare granulites are closely associated with these rocks. Significant amounts of metamorphosed terrigenous sediments (psammitic paragneisses) are present; these were mostly (>90%) derived from erosion of local Cadomian rocks and deposited in intra-arc and backarc basins (Shafaii Moghadam et al. 2017). Due to exhumation from the middle crust, most Cadomian basement rocks are deformed, and some have undergone partial melting and migmatization. Felsic rocks include arc-related I-type magmatic rocks with less abundant A-type granites and rhyolites, which are interpreted to have formed in a rearc environment. Metamorphosed dikes (now orthogneisses) are present.
2. Unmetamorphosed mafic to felsic volcanic rocks and dikes reflecting mostly bimodal magmatism. These rocks are reported from central Iran, near Zarand-Saghand, and as xenoliths in salt domes in SE Iran, United Arab Emirates, and NE Oman. These rocks show calc-alkaline, I-type, and A-type signatures.
3. Metasediments interbedded with volcanics and intruded by Cadomian plutons. These are thick (>1,000 m) sequences of terrigenous sedimentary rocks, evaporites, and dolomites known as the Morad and Rizu-Dezu series in SE and central Iran (Stocklin 1968), the Hormuz series in SE Iran (Stocklin 1968), and the Ara Group in Oman (Bowring et al. 2007). These metasediments are also stratigraphic equivalents of Tashk and Kahar volcano-sedimentary sequence (with glacio-sediments) formations from central Iran (Saghand) and N Iran, respectively (Etemad-Saeed et al. 2015, Ramezani & Tucker 2003).

Many geologic maps subdivide the Cadomian continental nucleus of central Iran into three blocks: Yazd, Tabas, and Lut (**Figure 5*a***). There is no significant difference between the basement rocks exposed in this region, so structural boundaries are unlikely to represent significant separations between the three tracts. For this reason, we recommend that such terminology be abandoned. In fact, the Cadomian nucleus is the most stable crust of Iran.

Ediacaran (Cadomian) salt domes are found in the southern Zagros (**Figure 5*a***). These provide a link to similar-age evaporite basins in Arabia and Oman. The three great salt basins of NE Arabia trend NNE-SSW, orthogonal to the trend of hypothesized Cadomian backarc basins (**Figure 8*a***). The two largest and westernmost basins can be traced on either flank of the Qatar Arch into the salt diapirs of the Zagros. These salt domes are unique probes of the shallow subduction zone beneath Iran and the subducted salt basins. We do not know how deep these basins may extend in the subduction zone, but salt diapirs can rise through only weak regions such as the Zagros Fold-and-Thrust Belt; they cannot rise through stronger lithosphere beneath the Outer Ophiolite Belt and the Sanandaj-Sirjan Zone to the north. Whatever their original extent, evaporite basins of NE Arabia and subducted counterparts beneath the Zagros provide further evidence of late Ediacaran extension so that these rift basins lay below sea level at 541–547 Ma (Smith 2012).

3.1.2. Paleozoic sedimentary rocks, igneous rocks, and suture. Three noteworthy aspects of Iran Paleozoic geology are its sedimentary and igneous rocks and the ophiolite that defines the northern suture south of the Turan platform (**Figure 5*b,d***). Paleozoic sedimentary rocks are mostly marine shales, sandstones, limestones, and dolomites. Important unconformities are found for Late Ordovician to Early Devonian (Caledonian) and Late Carboniferous (Variscan) time (Stocklin 1968), reflecting modest orogenies. Stocklin (1968) noted that the total thickness of Ediacaran through Paleozoic sediments is remarkably constant across Iran, from 3 to 4 km thick. This succession suggests that Iran mostly behaved as a marine platform during Paleozoic time.

Annu. Rev. Earth Planet. Sci. 2021.49:9-36. Downloaded from www.annualreviews.org
Access provided by University of Texas - Dallas on 06/01/21. For personal use only.

Annu. Rev. Earth Planet. Sci. 2021.49:9-36. Downloaded from www.annualreviews.org
Access provided by University of Texas - Dallas on 06/01/21. For personal use only.

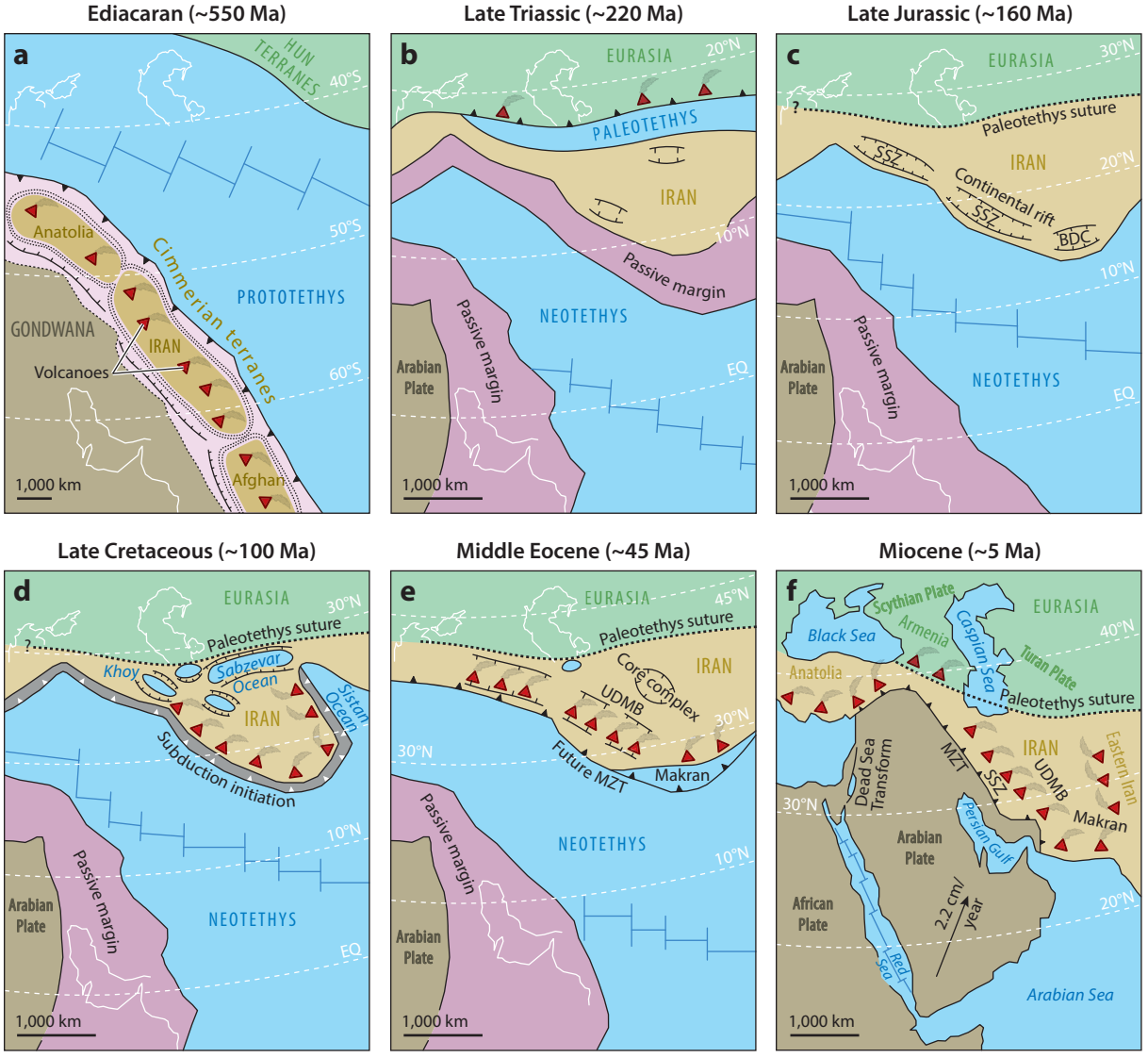

Figure 8

Paleogeographic maps. (*a*) Origin of Anatolia-Iran as an extensional magmatic arc on the N flank of Gondwana. (*b*) Northward drift and collision of Iran-Anatolia with Eurasia in Permian–Triassic time. (*c*) Early Mesozoic evolution. The southern margin of Iran was a passive continental margin and was affected by Jurassic rifting to form the SSZ. (*d*) Late Cretaceous subduction initiation on the S flank of Iran to form Zagros ophiolites and also backarc basin extensional zones. The Zagros Fold-and-Thrust Belt began as an accretionary prism at this time. (*e*) Evolution of Iran as a magmatically vigorous, extensional arc in Paleogene time, with continued growth of the Zagros Fold-and-Thrust Belt. (*f*) Start of collision with Arabia in early Neogene time, with waning arc magmatism. Abbreviations: BDC, Bajgan-Durkan Complex; MZT, Main Zagros Thrust; SSZ, Sanandaj-Sirjan Zone; UDMB, Urumieh-Dokhtar magmatic belt.

Paleozoic igneous rocks are not a major component of Iranian crust, but there are some, for example, 357–306 Ma (zircon U-Pb ages) gabbronorites and A-type granites in NW Iran (Shafaii Moghadam et al. 2015b) and ~450 Ma (Ordovician; zircon U-Pb ages) gabbros in NE Iran intruding Ordovician sedimentary rocks. Ordovician lavas are also present in NE Iran (the Soltan

Meidan basalts); these are thought to have erupted during rifting to open Paleotethys (Derakhshi et al. 2017).

Paleozoic ophiolites in northern Iran define the boundary between the Turan (Eurasia) block and Cimmeria (central Iran) where subduction beneath southern Eurasia consumed Paleotethys lithosphere, leading to Triassic collision that welded Iran to Eurasia (Shafaii Moghadam & Stern 2014). There are five well-known examples of middle to late Paleozoic ophiolitic remnants, aligned in two main zones in northern Iran: Aghdarband, Mashhad, and Rasht in the north, and Jandagh-Anarak ophiolites to the south (**Figure 5*d***). The Anarak, Jandaq, and Posht-e-Badam complexes of east-central Iran have been called the Variscan Accretionary Complex by Bagheri & Stampfli (2008). Paleozoic ophiolites have zircon U-Pb ages of 383–380 Ma and show both Sanandaj-Sirjan Zone– and mid-ocean ridge basalt–type mineralogical and geochemical signatures, perhaps reflecting formation in a marginal basin (Shafaii Moghadam et al. 2015b). Paleozoic ophiolites of Iran suggest a progression from oceanic crust formation above a subduction zone in Devonian time to accretionary convergence in Permian time.

3.1.3. Sanandaj-Sirjan Zone. The Sanandaj-Sirjan Zone is a distinctive ~150-km-wide belt that trends NW-SE for ~1,500 km along southern Iran inboard of the Zagros Fold-and-Thrust Belt and Outer Ophiolite Belt (**Figure 5*c***). The Sanandaj-Sirjan Zone includes magmatic and metamorphic rocks dominated by Jurassic phyllites, plutons, and metavolcanic rocks. Early Cretaceous limestones unconformably overlie deformed and intruded Jurassic rocks. The Sanandaj-Sirjan Zone also contains Cadomian crust, linking it to the Iran Cadomian nucleus.

Jurassic mafic and felsic igneous rocks and migmatites are abundantly exposed in the central Sanandaj-Sirjan Zone (**Figure 5*c***). Until recently, these igneous rocks were considered to represent an active Andean-like continental margin that formed as a consequence of Mesozoic convergence between the Afro-Arabian and Eurasian plates (Hassanzadeh & Wernicke 2016, and references therein). The interpretation of the Sanandaj-Sirjan Zone as representing a Jurassic magmatic arc was largely based on the linear nature of the magmatic belt and the arc-like geochemical features of some igneous rocks. However, this model is challenged with an alternative interpretation that the Sanandaj-Sirjan Zone formed as a continental rift (Azizi & Stern 2019, Hunziker et al. 2015). The new interpretation emphasizes that Jurassic magmatism did not continue all along the Sanandaj-Sirjan Zone for a protracted time (tens of millions of years, as would be expected for a magmatic arc above a subduction zone) but that the locus of magmatism migrated NW along the Sanandaj-Sirjan Zone from ~175 Ma to ~145 Ma at a rate of ~20 mm/year. Arc magmatism does not do this, but rifts and hotspots do. The arc-like nature of some Jurassic Sanandaj-Sirjan Zone igneous rocks was interpreted by Azizi & Stern (2019) on the basis of geochemical and isotopic data as due to strong contamination of juvenile mantle melts by Iranian continental crust. Interpretation of the Sanandaj-Sirjan Zone as a Jurassic rift is also favored by thick sequences of Early Cretaceous limestone, which are significantly thicker here than elsewhere in Iran, most likely due to thermal subsidence of rifted continental lithosphere.

The Sanandaj-Sirjan Zone continues S-SE to connect with the Bajgan-Durkan metamorphic complex of Makran. The Bajgan-Durkan complex differs from the Sanandaj-Sirjan Zone in containing fewer Jurassic intrusions (Hunziker et al. 2015). The Bajgan-Durkan complex is up to 40 km wide and consists of Permian and Late Jurassic limestones and marbles that are overlain by Mesozoic shelf carbonates (McCall 1985). The Bajgan complex includes amphibolites, marbles, calc-silicate rocks, and schists with meta-volcanic rocks and mafic to felsic intrusive rocks. The Durkan complex is mainly composed of Paleozoic detritus rocks as well as Mesozoic shelf carbonates, sandstones, and argillic rocks with interbedded lavas and small mafic intrusions. The Durkan complex also contains tectonic inliers of Carboniferous, Permian, and Jurassic shelf limestones.

Annu. Rev. Earth Planet. Sci. 2021.49:9-36. Downloaded from www.annualreviews.org
Access provided by University of Texas - Dallas on 06/01/21. For personal use only.

Pillow lavas, cherts, lapilli tuffs, and minor mafic-ultramafic intrusions are also common (McCall 2002).

The Sanandaj-Sirjan Zone controversy is likely to persist for some time, but it is important to resolve because the hypothesis that an episode of subduction initiation occurred in Late Cretaceous time along the SW margin of Eurasia from Oman to Cyprus (Shafaii Moghadam & Stern 2011) depends on understanding the tectonic setting of Jurassic magmatism in the Sanandaj-Sirjan Zone. If the Jurassic Sanandaj-Sirjan Zone was a magmatic arc, then the Late Cretaceous subduction initiation hypothesis is much less compelling. If, however, the propagating rift model is a better approximation of reality, then the subduction initiation model is strengthened. Such a resolution has essential implications for reconstructing Mesozoic plate motions as well as providing the first example of a Mesozoic passive continental margin collapsing to form a new subduction zone.

Annu. Rev. Earth Planet. Sci. 2021.49:9-36. Downloaded from www.annualreviews.org
Access provided by University of Texas - Dallas on 06/01/21. For personal use only.

3.1.4. Mesozoic sedimentary rocks. There are thick sequences of Triassic, Jurassic, and Cretaceous shallow epicontinental to deep-sea sedimentary rocks in nearly all parts of Iran (Berberian & King 1981). Because of Iran's geodynamic evolution, these are usefully subdivided into Triassic (deposited during accretion of Iran to Eurasia), Jurassic–Early Cretaceous (deposited during Sanandaj-Sirjan Zone rifting), and Late Cretaceous (deposited during and after subduction initiation) sequences. These three sequences are discussed further below.

3.1.4.1. Triassic rocks. Lower to Middle Triassic sedimentary rocks in Iran comprise carbonate rocks built on the shelves of the Paleo- and Neotethys Oceans (**Figure 8*b***). The depositional environments varied from shallow marine to lagoonal and near-shore tidal flats, locally evaporitic. Late Triassic carbonates are found only in SW Iran in the Sanandaj-Sirjan Zone. Thick siliciclastic and molassic sediments in central Iran were deposited due to the closure of the Paleotethys and Iran-Turan collision. Thick sequences of Triassic volcaniclastic and basinal sediments found near Anarak in central Iran and near Aghdarband in NE Iran have been interpreted as remnants of the northern Paleotethys margin (Seyed-Emami 2003).

Triassic igneous rocks are rare in Iran and occur only as small plutons and dikes that locally intrude Cadomian crust. Late Triassic granites (zircon U-Pb ages of 212–217 Ma) outcropping in NE Iran are interpreted as syn- to postcollisional intrusions formed as a result of Iran-Turan collision (Mirnejad et al. 2013).

3.1.4.2. Jurassic–Early Cretaceous rocks. Jurassic sedimentary rocks are abundant throughout Iran, comprising mostly shale and sandstones with thin carbonates. These are called the Shemshak Formation in central Iran and are equivalent to the Hamadan phyllites in the Sanandaj-Sirjan Zone. Jurassic sedimentary rocks also contain thick coal layers. Jurassic igneous rocks are widespread in the Sanandaj-Sirjan Zone but are rare elsewhere in Iran (**Figure 5*c***).

Thick sequences of Early Cretaceous carbonate rock are ubiquitous throughout Iran. In NE Iran, the Lower Cretaceous limestones are interlayered with tuffs and pillow lavas. Early Cretaceous igneous rocks are abundant in the northern Sanandaj-Sirjan Zone but are also found in the southern Sanandaj-Sirjan Zone near Haji-Abad (**Figure 5*c***), where they are interlayered with Lower Cretaceous limestones.

3.2. Late Cretaceous–Cenozoic Igneous and Sedimentary Rocks

Late Cretaceous–Cenozoic rocks comprise the third geotectonic domain of Iran. This group is distinguished because these rocks were deposited after the present tectonic episode began. Four units

are important: (*a*) Mesozoic (mostly Late Cretaceous) ophiolites, (*b*) Late Cretaceous–Cenozoic arc volcanics and plutons, (*c*) Cenozoic sedimentary basins and metamorphic core complexes, and (*d*) Pliocene–Quaternary volcanoes.

3.2.1. Mesozoic ophiolites and ophiolite belts. Iran is laced with Mesozoic ophiolite belts (**Figure 5*d***); these can be subdivided into six subgroups: (*a*) Outer Zagros Ophiolite Belt, (*b*) Inner Zagros Ophiolite Belt, (*c*) Makran ophiolites, (*d*) NE Iran ophiolites, (*e*) NW Iran ophiolites, and (*f*) eastern Iranian Ophiolite Belt. These are all associated with subduction initiation on the southern margin of Euarasia ~100 Ma. The idea that Late Cretaceous ophiolites of Iran formed during a subduction initiation episode on the SW margin of Eurasia is relatively new. Subduction initiation requires the sinking of one plate beneath another, and this exerts extension stress on the overlying plate. How broad a region is affected by subduction initiation–related extension is unclear because most subduction initiation examples are deep under the ocean, but in the case of Iran, extension affected a region up to 1,000 km across. Each of these ophiolite belts is discussed briefly below.

The Outer Ophiolite Belt trends discontinuously NW-SE between the Zagros Fold-and-Thrust Belt to the southwest and the Sanandaj-Sirjan Zone to the northeast. The Outer Ophiolite Belt continues southeast into the Makran ophiolite belt (**Figure 5*d***). The Main Zagros Thrust separates Outer Ophiolite Belt ophiolites from the Zagros Fold-and-Thrust Belt. The Outer Ophiolite Belt is the SW limit of crystalline Iran crust and acts as a backstop to the Zagros Fold-and-Thrust Belt. The Outer Ophiolite Belt also serves as part of the inner Iran forearc for the Zagros accretionary prism, which occupies an outer forearc position. Outer Ophiolite Belt ophiolites are exposed around Kermanshah, Neyriz, and Haji-Abad (Esfandagheh). U-Pb ages for zircons from plagiogranites in the Kermanshah and Neyriz ophiolites indicate that these formed during the Late Cretaceous (Monsef et al. 2018, Shafaii Moghadam & Stern 2015).

The Inner Ophiolite Belt of Late Cretaceous ophiolites extends NW-SE for 500–600 km on the NE flank of the southern Sanandaj-Sirjan Zone and includes, from NW to SE, the Nain, Dehshir, and Baft ophiolites. This ophiolite belt bends northeast before being buried beneath the arid Dasht-e Kavir and may link up with NE Iran ophiolites. These ophiolites occur as nappes that were imbricated during Late Cretaceous time and crosscut by younger strike-slip faults. U-Pb zircon ages indicate that the Nain, Dehshir, and Baft ophiolites formed at ca. 103–99 Ma (Shafaii Moghadam & Stern 2015). The Outer Ophiolite Belt and Inner Ophiolite Belt formed on opposite flanks of the Sanandaj-Sirjan Zone described below.

There are abundant Late Cretaceous ophiolites in NE Iran. The main outcrops occur near the cities of Sabzevar and Torbat-e-Heydarieh (**Figure 5*d***). These ophiolites, which have zircon U-Pb ages of 100–78 Ma, formed in a backarc basin separated from the Zagros forearc Outer Ophiolite Belt and Inner Ophiolite Belt by the central Cadomian nucleus (Shafaii Moghadam et al. 2014). Late Cretaceous ophiolites are also found in NW Iran near Khoy and Maku (**Figure 5*d***). These are bounded by the Cadomian crustal nucleus of Iran on the east and by Anatolian crust to the west. Biostratigraphic data from limestones interlayered with ophiolitic pillow lavas indicate a Late Cretaceous age (Khalatbari-Jafari et al. 2006).

Cretaceous ophiolites are also found in eastern Iran (**Figure 5*d***) associated with an ~400-km-long accretionary prism and a forearc basin. These N-S-trending ophiolites define the Sistan Suture Zone and demarcate the boundary between the Iranian Cadomian crustal nucleus and the Afghan continental block. Radiolarites from these ophiolites are characterized by early Aptian and middle late Albian faunas (Babazadeh & De Wever 2004), suggesting that these ophiolites are significantly older than the Late Cretaceous ophiolites to the west. The eastern Iran accretionary prism comprises Cretaceous ophiolites (**Figure 5*d***) overlain by early

Annu. Rev. Earth Planet. Sci. 2021.49:9-36. Downloaded from www.annualreviews.org
Access provided by University of Texas - Dallas on 06/01/21. For personal use only.

Aptian to Maastrichtian pelagic sediments, Late Cretaceous–Eocene clastic sediments, and Late Cretaceous–early Eocene unmetamorphosed marine sandstone and marly turbidites. Deep-water sedimentation continued until early Eocene time. The forearc basin includes Cenomanian–Eocene clastic deposits with deep-marine carbonates and Late Cretaceous–Eocene calc-alkaline lavas (Camp & Griffis 1982, Tirrul et al. 1983) (**Figure 5*e***). Subduction-related blueschists, eclogites, and other metamorphic rocks associated with Birjand ophiolites give Early to Late Cretaceous white mica $^{39}Ar/^{40}Ar$, Rb-Sr, and zircon U-Pb radiometric ages (Bröcker et al. 2013).

Recent studies (e.g., Monsef et al. 2018) assign Jurassic to Late Cretaceous ages to the Makran ophiolites in SE Iran and relate these to the ~96 Ma Semail ophiolite in northern Oman and the United Arab Emirates (Guilmette et al. 2018). However, the Makran and Semail ophiolites are presently separated by the Makran convergent plate boundary. Further research is needed to better understand the relationship between Makran ophiolites and the Semail, SW Pakistan, Birjand, and Zagros ophiolites. Another curious feature is that some Makran ophiolites contain zircons with Cadomian U-Pb ages (Sepidbar et al. 2020)—is this inheritance or geologic complexity? Emplacement of the Late Cretaceous ophiolites of Iran was most likely a response to a major tectonic change following the strongly extensional lithospheric stress regime associated with Late Cretaceous subduction initiation along the SW flank of Iran's Cadomian nucleus (**Figure 5*d***).

Because old oceanic lithosphere is strong as well as dense, collapse and subduction initiation require an extensive (>1,000-km long) lithospheric weakness (Stern & Gerya 2018). Subduction initiation caused a broad zone of upper plate extension to the point of seafloor spreading and ophiolite formation. This process has been described by many workers, most recently by Arculus et al. (2019). More research is needed to test and refine models of the Late Cretaceous subduction initiation in Iran and emplacement of the ~2,000-km-long ophiolite belt extending from Oman to Cyprus and to understand what the Late Cretaceous ophiolites of Iran reveal about Late Cretaceous subduction initiation along the SW flank of Eurasia.

3.2.2. Late Cretaceous–Cenozoic arc volcanics and plutons. Late Cretaceous–Cenozoic rocks of Iran include erosional remnants of plutons, lavas, and sediments found north of the Zagros Fold-and-Thrust Belt. These rocks formed as part of the continental magmatic arc that was established after an N-dipping subduction zone formed beneath Iran in Late Cretaceous time. The Iran arc is an Andean-type magmatic arc that differs significantly from the Andes because the former was extensional and the latter is contractional. The extensional nature of the Paleogene Urumieh-Dokhtar magmatic belt is further demonstrated by evidence that eruptions occurred near sea level, as shown by abundant shallow marine sediments across Iran (Berberian & King 1981). Magmatism was likely enhanced by regional extension, and Eocene extension and igneous activity were especially strong. The cause of Neogene igneous activity after the Arabia-Iran collision began is more enigmatic, partly because it is unclear whether a subducted slab now exists beneath Iran (**Figures 3** and **4**) and, if not, how long this situation has existed. Other possible causes of Neogene igneous activity include delamination of the base of the overriding plate and slab breakoff.

Many magmatic arcs are narrow, 100–200 km across (Stern 2002), but the Iran magmatic arc is much wider, up to 1,000 km from north to south. Late Cretaceous–Cenozoic igneous rocks are especially abundant as part of the NW-SE-trending Urumieh-Dokhtar magmatic belt, which defines the arc magmatic front (**Figure 5*e***). Similar-age igneous rocks are also abundant in northern Iran from Azerbaijan through Alborz and east into the region south of Kopet Dagh as part of the reararc.

Annu. Rev. Earth Planet. Sci. 2021.49:9-36. Downloaded from www.annualreviews.org
Access provided by University of Texas - Dallas on 06/01/21. For personal use only.

Late Cretaceous–Cenozoic igneous rocks are also abundant in a N-S belt in eastern Iran (**Figure 5*e***). Some of these may be related to westward subduction of Sistan oceanic lithosphere (**Figure 5*d*,*e***).

Below we subdivide the Cenozoic Iran arc into magmatic front and rearare magmatic belt and discuss these in more detail. We also discuss the Cenozoic magmatic rocks from eastern Iran and Makran separately.

3.2.2.1. Magmatic front. The Urumieh-Dokhtar magmatic belt is 50–80 km wide and trends NW-SE for more than 1,000 km across Iran between 28° and 39°N. It defines the magmatic front of the Iran arc. Urumieh-Dokhtar magmatic belt magmatism was very active in Paleogene time and has since waned. Because it evolved as an extensional arc, Urumieh-Dokhtar magmatic belt products and thus the history of subduction-related igneous activity are well-preserved. Urumieh-Dokhtar magmatic belt igneous activity started in Late Cretaceous time with eruption of low-K tholeiitic and calc-alkaline magmas and evolved into a mature arc in the Paleogene. A short magmatic lull in the early Paleocene was followed by a change to calk-alkaline volcanism in the middle to late Paleocene. The Urumieh-Dokhtar magmatic belt was especially active from Eocene to Miocene time (ca. 55–5 Ma), with some episodes of high magmatic flux (flare-ups) (Ducea & Barton 2007) during the Eocene, before changing magmatic style as a result of Arabia-Iran collision beginning in late Oligocene–Miocene time. Eocene magmatic flare-up occurred during a time of strong extension during which several metamorphic core complexes were exhumed (Verdel et al. 2011) (**Figure 5*f***).

The Urumieh-Dokhtar magmatic belt volcanic succession includes thick (~4 km) sequences of calc-alkaline, shoshonitic, and adakitic lavas and pyroclastic rocks. Calc-alkaline and shoshonitic igneous rocks are especially abundant. These igneous rocks formed as compositionally distinct pulses. Abundant early to middle Eocene volcanic rocks have high-K calc-alkaline signatures. Magmas became shoshonitic during late Eocene to Oligocene and ultrapotassic in Miocene time. Late Miocene to Pliocene–Quaternary Urumieh-Dokhtar magmatic belt volcanic rocks have adakitic and alkaline (ocean island basalt–like) geochemical signatures (Deevsalar et al. 2017, Kheirkhah et al. 2015, Neill et al. 2015).

Urumieh-Dokhtar magmatic belt plutonic rocks have Late Cretaceous to Miocene ages. Eocene–Oligocene to Miocene plutonic rocks are most abundant (**Figure 5*e***) and have calc-alkaline to high-K calc-alkaline signatures (Babazadeh et al. 2017). Nearly all of these plutons are barren in mineralization. Mineralized Miocene intrusive rocks occur in the SE Urumieh-Dokhtar magmatic belt, from Dehshir to Bam (Asadi et al. 2014) (**Figure 5*e***). Melting of asthenospheric (Babazadeh et al. 2017) or lithospheric mantle (Asadi et al. 2014) and/or melting of the subducted Arabian plate (Mirnejad et al. 2018) along with variable contamination by Iran Cadomian crust is suggested to be responsible for generating Urumieh-Dokhtar magmatic belt Oligocene to Miocene plutonic rocks.

3.2.2.2. Rearare magmatic belt. Rearare igneous activity occurred along an E-W-trending belt (>1,200 km long) (**Figure 5*e***) during the latest Cretaceous to Miocene, with eruption of marine to subaerial magmatic rocks, including thick sequences of marine pyroclastic rocks (Ballato et al. 2011, Verdel et al. 2011). This magmatism developed in response to Paleogene extension and crustal thinning. Several transgression-regression cycles are also recorded in latest Cretaceous to Eocene rearare sediments (Ballato et al. 2011) (**Figure 5*e*,*f***).

Late Cretaceous–Neogene magmatism across the Iran arc—both magmatic front and rearare—is remarkably heterogeneous in composition and petrological characteristics. Volcanic rocks are abundant in the Iran rearare. Volcanic rocks of intermediate to acidic composition—often

Annu. Rev. Earth Planet. Sci. 2021.49:9-36. Downloaded from www.annualreviews.org
Access provided by University of Texas - Dallas on 06/01/21. For personal use only.

pyroclastic—dominate along the magmatic front, although mafic volcanic rocks are also found. In contrast, mafic volcanic rocks are more abundant in the Iran rearc than are felsic rocks. Shoshonitic to ultrapotassic rocks are mostly restricted to the rearc (Asiabanha & Foden 2012, Castro et al. 2013, Ghorbani et al. 2014, Shafaii Moghadam et al. 2018). Iran rearc Late Cretaceous sequences are mostly marine, comprising rhyolitic to dacitic (with rare andesitic) lavas, felsic tuffs, and radiolarites. Subaerial lavas including alternating basalts and dacites are also common. These are overlain by both middle Paleocene–Eocene terrigenous sediments and mid–late Paleocene–Eocene acidic to intermediate pyroclastic rocks with intercalated mafic to andesitic lavas. Eocene lavas were mostly deposited in shallow marine environments.

Several plutonic pulses accompanied Iran rearc volcanism. In NE Iran, Late Cretaceous–Paleogene plutonic rocks with low-K tholeiitic to calc-alkaline signatures intrude thick sequences of Cretaceous terrigenous sediments as well as pyroclastic rocks and lavas. Eocene rearc intrusive rocks vary from calc-alkaline to adakitic in NE Iran to Na-rich alkaline intrusions in NW Iran (Ashrafi et al. 2018). Late Eocene–Oligocene to Miocene plutonic rocks are abundant in the NW Iran rearc and have high-K calc-alkaline to shoshonitic signatures (Castro et al. 2013). Eocene high-K calc-alkaline intrusive rocks are also found in the N Iran rearc (Sepidbar et al. 2018).

Annu. Rev. Earth Planet. Sci. 2021.49:9-36. Downloaded from www.annualreviews.org
Access provided by University of Texas - Dallas on 06/01/21. For personal use only.

3.2.2.3. Eastern Iran. Eastern Iran is characterized by an ~400-km-long ophiolite belt, an accretionary prism with high-pressure/temperature metamorphic rocks, and a forearc basin, as described in Section 3.2.1. The eastern Iran accretionary prism comprises Cretaceous ophiolites (**Figure 5*d***) overlain by early Aptian to Maastrichtian pelagic sediments, Late Cretaceous–Eocene clastic sediments, and Late Cretaceous–early Eocene unmetamorphosed marine sandstone and marly turbidites. The forearc basin includes Cenomanian to Eocene clastic deposits with deep-marine carbonates and Late Cretaceous to Eocene calc-alkaline lavas (Camp & Griffis 1982, Tirrul et al. 1983) (**Figure 5*e***). Eastern Iran forearc sediments are covered by Eocene–Oligocene calc-alkaline to shoshonitic extrusive rocks. Westward subduction of the Birjand (or Birjand-Sistan) oceanic lithosphere beneath the Lut block is sometimes suggested to have triggered Cretaceous and Cenozoic magmatic activity. However, Paleogene magmatism postdates collision between the Lut and Sistan blocks in latest Cretaceous time and cannot be related to westward subduction and closing of the Sistan Ocean. Pang et al. (2013) proposed that Paleogene magmatism in the Birjand-Zahedan magmatic belt was triggered by convective removal of lithosphere (delamination) and resultant asthenospheric upwelling accompanying extensional collapse. However, these igneous rocks lie between the Urumieh-Dokhtar magmatic arc and Iran rearc and are more likely to be related to Arabian plate subduction. Asthenospheric upwelling may be responsible for middle Miocene alkali basaltic volcanism (^{40}Ar-^{39}Ar age 14–11 Ma) (Pang et al. 2012).

3.2.2.4. Makran magmatic belt. The Makran magmatic belt (SE Iran) is an E-W magmatic belt with four large and young stratovolcanoes: Koh-i-Sultan in Pakistan and the Taftan, Kuh-e-Nadir, and Bazman volcanoes of Iran. U-Pb zircon ages of 7.5 to 0.84 Ma are reported for lavas from these volcanoes (Pang et al. 2014). The Makran magmatic belt reflects subduction of oceanic lithosphere beneath SE Iran (**Figure 3**). Paleogene igneous rocks are not reported from the Makran magmatic belt, the lack of which may be due to erosion, as represented by abundant Paleogene turbidites (Burg 2018), or may be due to low-angle or flat-slab subduction of the Arabian plate beneath Makran (Abedi & Bahroudi 2016).

3.2.3. Cenozoic sedimentary basins and metamorphic core complexes. Cenozoic basins of Iran include extensional and compressional basins. Metamorphic core complexes formed during

episodes of strong extension (Martinez et al. 2001). The Golpayegan and Saghand core complexes of central Iran formed in the Eocene, the Takab core complex of NW Iran formed in the Oligocene, and the Torud core complex is suggested to have formed in Late Cretaceous–Eocene time (Malekpour-Alamdari et al. 2017, Moritz et al. 2006, Verdel et al. 2007). Late Cretaceous extension was likely related to subduction initiation along the southern margin of Eurasia and was accompanied by backarc basin formation in NE Iran (see Section 3.2.1). Mesozoic extension was also intense around the Main Zagros Thrust and formed deep basins that were filled with hundreds of meters of pillow basalts, deep marine pelagic sediments, and Urumieh-Dokhtar magmatic belt volcanic detrital sediments. Such basins are known in W Iran in the region from Kermanshah to Iraqi Kurdistan; these accumulated sequences are known as the Walash-Naopurdan sequence in Iraqi Zagros (Ali et al. 2013).

Latest Cretaceous–early Paleocene transition from extension to compression resulted in the closing of backarc basins and uplift of NE Iran backarc basin ophiolites. Mid- to Late Paleocene regression led to deposition of red volcano-sedimentary sequences. Eocene time witnessed resumed extension in the Iranian Plateau, perhaps due to rollback of the Neotethys slab, resulting in a marine transgression over most of Iran. The early to middle Eocene transgression in NE Iran is represented by thick (500–1,000 m) sequences of deep marine Nummulite-bearing limestone (Shafaii Moghadam et al. 2015a). These limestones grade into volcaniclastics with intercalated andesitic lavas.

A remarkable example of very strong Paleogene extension is a more than 220-km-long magmatic forearc rift that formed ca. 40–37 Ma (Shafaii-Moghadam et al. 2020b). This outcrops along the Iran-Iraq border from southeast of Kermanshah (Iran) to Hasanbag (Iraq) (**Figure 1**). A thick pile (>1,000 m) of mid-ocean ridge basalt–like pillow lavas and pelagic sediments is overlain by and/or interlayered with Paleogene sandstones and pelagic limestones. Gabbros, granites, and dikes but not mantle rocks are associated with pillow lavas and sediments. Field observations indicate that Paleogene rocks were injected into and/or underlain by Late Cretaceous Zagros forearc ophiolites, the Kurdistan-Kermanshah ophiolites.

3.2.4. Pliocene–Quaternary volcanoes. Pliocene–Quaternary volcanism across Iran shows variable geochemical compositions including adakitic, alkaline (ocean island basalt–like), shoshonitic, and ultrapotassic. According to the Smithsonian Global Volcanism Program, Iran has six active and dormant volcanoes. These occur in two groups of three volcanoes, one in the northwest and the other in the southeast (**Figure 1**). The SE group consists of three arc volcanoes related to Makran subduction: Bazman, Kuh-e-Nadir, and Taftan. The NW group consists of Damavand (a trachyandesite rearc volcano near the Caspian Sea), Sabalan (an adakitic andesite, trachyandesite, dacite, and rhyolite rearc volcano southwest of the Caspian Sea), and Sahand (an adakite volcano in NW Iran west of Sabalan). There are also slightly older (Pliocene–Quaternary) shoshonitic stratovolcanoes such as Kuh-e-Mozahim in Shahr-e-Babak (Kerman) and also Quaternary ultrapotassic maar-like volcanoes such as Qal'eh Hasan Ali in SE Iran near Kerman (Pang et al. 2015) and/or Quaternary adakitic domes (Pang et al. 2016), which are found in several places.

3.3. Zagros Fold-and-Thrust Belt

The Zagros Fold-and-Thrust Belt (**Figures 5*d*** and **7**) is up to 300 km wide and extends for nearly 2,000 km from southeastern Turkey through northern Syria, northeastern Iraq, and western and southern Iran; comparable units can be traced into the Makran and Pakistan as far east as the N-S Chaman Fault. The Zagros orogen consists of two related tectonic zones oriented parallel to the

Annu. Rev. Earth Planet. Sci. 2021.49:9-36. Downloaded from www.annualreviews.org
Access provided by University of Texas - Dallas on 06/01/21. For personal use only.

Arabian-Eurasian plate boundary: yet-to-be accreted sediments of the Mesopotamian Foredeep and the Persian Gulf and accreted, deformed wedge-top sediments in the High Zagros and Simply Folded Zagros (Pirouz et al. 2011). The continued northward movement of the Arabian plate and convergence with Iran results in uppermost Arabian plate sediments being progressively scraped off and added to the outermost Zagros Fold-and-Thrust Belt. The Zagros Fold-and-Thrust Belt records the history of this off-scraping, with the oldest additions found in the northeast and the youngest additions in the southwest (**Figures 5*c*** and **7**). In many respects, the Persian Gulf and the Mesopotamian Foredeep behave like a sediment-filled oceanic trench, and the Zagros Fold-and-Thrust Belt is thus the accretionary wedge (Farhoudi & Karig 1977). Most accretionary wedges elsewhere around the world are deeply submerged beneath the sea, making the Zagros Fold-and-Thrust Belt of global geoscientific significance.

Arabian continental crust was mapped beneath the Zagros by Hatzfeld et al. (2003) using arrival times of local events and receiver functions for a dense seismological network. They found that this region consists of 11 km of thick sedimentary rocks underlain by thin (8 km) upper continental crust above a 27-km-thick lower crust of 6.5 km/s P-wave velocity. The total thickness (~35 km) of the crust is similar to that of the stretched margin of the Arabian platform. Total shortening of the Zagros Fold-and-Thrust Belt inferred from sedimentary cover varies between 50 and 65 km across the Zagros, while a three-dimensional volumetric reconstruction of crust thickness shows about 125 km of average shortening. It is worth noting that the modern Zagros foreland basin architecture (e.g., location of the foredeep and bulge of the foreland system) needs at least 350 km of total shortening to be accommodated in the Zagros Fold-and-Thrust Belt, which agrees with estimated timing of collision and average plate velocity since collision (Pirouz et al. 2017). Salt diapirs, derived from Ediacaran evaporites on the downgoing Arabian plate, intrude the southern Zagros (**Figure 5*a***).

4. DISCUSSION

Iran is an outstanding example of an active orogen with a well-defined tectonic history. Over its 600-million-year history, it has evolved from a continental arc to a rifted continental sliver to an accreted terrane with a passive continental margin to a convergent plate margin, and it is now in the early stages of continental collision. Iran's tectonic evolution is simplified into six stages in **Figure 8**. In the first panel (**Figure 8*a***), the crustal nucleus of Iran (and Anatolia) was generated by a very vigorous (Cadomian) magmatic arc on the northern margin of Gondwana, above an S-dipping subduction zone. The Cadomian arc was strongly extensional, opening a backarc basin that by the end of Paleozoic time widened into the Rheic Ocean south of the northward-drifting Cimmeria microcontinent (Iran-Anatolia). The southern flank of Iran was a passive continental margin (**Figure 8*b***). Cimmeria collided with Eurasia in Permian–Triassic time. In the Jurassic, a magmatic rift formed near the SW margin of Iran; this is known as the Sanandaj-Sirjan Zone (**Figure 8*c***). Jurassic rifting created a lithospheric weakness that allowed Tethys oceanic lithosphere to collapse in Late Cretaceous time to form an N-dipping subduction zone. Late Cretaceous subduction initiation (**Figure 8*d***) was accompanied by strong extension that resulted in forearc spreading, backarc basin opening, and exhumation of some core complexes as well as causing a lot of igneous activity across the Iranian Plateau. The new convergent plate margin evolved into an extensional and strongly magmatic arc throughout Paleogene time (**Figure 8*e***), and the Zagros Fold-and-Thrust Belt began to grow as sediments were continuously scraped off subducted Tethyan seafloor. About 25 million years ago, Arabia rifted off the NE flank of Africa and soon began underthrusting Iranian continental lithosphere (**Figure 8*f***).

Annu. Rev. Earth Planet. Sci. 2021.49:9-36. Downloaded from www.annualreviews.org
Access provided by University of Texas - Dallas on 06/01/21. For personal use only.

Annu. Rev. Earth Planet. Sci. 2021.49:9-36. Downloaded from www.annualreviews.org
Access provided by University of Texas - Dallas on 06/01/21. For personal use only.

The timing of the Arabia-Eurasia collision has long been debated. Part of the challenge is knowing when the collision began because the two plates have been converging at the same rate (2–3 cm/year) for at least the past 56 Ma (McQuarrie et al. 2003). In the 1970s, early workers proposed a collisional age of Arabia and Iran of about 5 Ma. However, a decade later, other authors argued that the collision occurred earlier, between 20 and 45 Ma (e.g., Dercourt et al. 1986). In the past decade, a consensus has been reached that continental collision began sometime between 20 and 35 Ma (e.g., Agard et al. 2011, Ballato et al. 2011, Fakhari et al. 2008, Koshnaw et al. 2018, Mouthereau et al. 2012, Saura et al. 2015). Pirouz et al. (2017) suggest a narrower collisional time range (27 ± 2 Ma) on the basis of the oldest foreland deposits preserved above the forebulge unconformity near the suture and chronostratigraphy of the orogenic wedge loading. Variations of collisional age along the strike of the orogen are likely. It is plausible that collision in the northern Arabian margin and rifting on its south are linked and that the slab pull force on the NE flank of Afro-Arabia was sufficiently large to cause it to rupture and Arabia to separate along a zone of lithospheric weakness caused by the Afar plume.

Arabia did not slow its northward movement when it began to collide with Iran, in contrast to the case of India colliding with Asia, where a sharp deceleration of India at 50–55 Ma is thought to mark the beginning of collision (van Hinsbergen et al. 2011). Despite ~27 Ma of continental collision, the gross structure of the Iranian convergent margin has remained essentially intact. For these two reasons Iran-Arabia and India-Asia can be used as contrasting examples of soft and hard continental collisions.

Although estimates of Iranian crustal thickness vary widely, most do not indicate significant crustal thickening. Another indication of a soft collision is that all the elements of a normal convergent margin are preserved. For example, the Iran-Arabia plate boundary is marked by a well-defined trench-like foredeep (Mesopotamia and the Persian Gulf), accretionary prism (the Zagros Fold-and-Thrust Belt), inner forearc crust (Late Cretaceous ophiolites and the Sanandaj-Sirjan Zone), and remnants of a once-vigorous magmatic arc (the Urumieh-Doktar magmatic belt).

Preservation of the main elements of the Iranian convergent plate margin after 27 Ma of collision with Arabia contrasts with the obliteration of analogous features in the India-Asia collision zone, where the original forearc-arc elements of the southern Tibet convergent plate boundary marked by the Indus-Tsangpo suture lie several hundred kilometers north of the zone of active thrusting and maximum relief (the Himalayas). One explanation for the difference between Arabia-Iran soft collision and India-Tibet hard collision is the collision duration. Arabia-Iran convergence has been underway for half as long as India-Tibet (27 versus 55 Ma). Along the India-Asia plate boundary, significant shortening and associated topographic uplift of the Himalayas did not occur until ~25 Ma, about 30 million years after collision began (e.g., Ding et al. 2017). Thus, the India-Asia collision may have experienced ~30 Ma of soft collision before evolving ~25 Ma into the hard collision seen today, suggesting that a similar evolution may be in store for Iran in the future. Alternatively, Arabian lithosphere may be less buoyant than Indian lithosphere, allowing it to continue subducting without evolving into a hard collision. The key unknowns are the relative densities of Arabian versus Indian continental lithospheres: If they are similar, then a similar evolution from soft to hard collision is predicted; if the eastern Arabian lithosphere is denser (as suggested by Stern & Johnson 2010), then continued soft collision and partial or complete subduction of Arabia is more likely.

5. CONCLUSIONS AND FUTURE RESEARCH DIRECTIONS

Iran is a remarkable example of a convergent margin in the early stages of continent-continent collision. Although previous researchers have provided much insight into the nature and formation

of Iranian lithosphere, additional studies are necessary in order to fully understand the geodynamic evolution of Iran. The list below summarizes what we view to be some of the most important avenues for future research:

1. We need to investigate lateral variations in the thickness and physical properties of the upper mantle beneath Iran in order to better understand the fate of the subducted Arabian lithosphere. If the Arabian plate first collided with Iran 25 Ma and has converged at ~30 mm/year, then ~750 km of Arabian continental lithosphere lies beneath Iran. As noted above, there is a lack of deep seismicity beneath Iran and Anatolia for 2,500 km west of the Makran subduction zone. Does this lack of seismicity represent the western edge of oceanic lithosphere subducted beneath Makran? Alternatively, does the Neband-Minab fault (**Figure 6**) mark the surface expression of a tear between the Makran slab and aseismic subducted Arabian lithosphere to the west? Although many researchers hypothesize that the subducted Arabian lithosphere has broken off, there is insufficient geophysical evidence to confirm or refute this assertion. We need a geophysical experiment designed to detect subducted or broken-off Arabian lithosphere or delaminated Iranian lithosphere. We also need to better understand the lateral variations in physical properties of Iranian lithosphere. Existing seismic tomography reveals that much of the upper mantle beneath Iran has low seismic wave speeds, indicating that it is unusually warm, fluid-rich, or both. A series of SW-NE-oriented passive-source seismic profiles could resolve the lithosphere-asthenosphere boundary beneath Iran. Robust seismic images of the P-wave and S-wave structures of the uppermost mantle beneath Iran are also called for. Studies of upper mantle xenoliths would significantly enhance current understanding of the lithosphere beneath Iran.
2. We need to better image Iranian crustal thickness and understand its velocity structure. To do this we need both refraction and ambient seismic noise experiments, the former optimally oriented NNE-SSW across central Iran. Studies of crustal xenoliths would help advance our understanding of Iran crustal structure and evolution.
3. The origins of salt diapirs and hydrocarbons in the Zagros Fold-and-Thrust Belt provide unique perspectives on mass transfer between the subducting and overriding plates. The northern limit of salt domes may reveal a fundamental boundary between crust that is weaker than a rising salt diapir in the Zagros to the south and stronger lithosphere to the north. Research is needed to better understand what this is telling us about the structure and operation of the shallow (<50-km deep) subduction zone of this region. Research on how deep oil and salt can be subducted and still survive, and what if any impact subduction of salt and oil may have on the composition of the overlying arc magmas, should be carried out. Most Iranian hydrocarbon deposits are found in the Zagros Fold-and-Thrust Belt. Did these deposits also originate in the downgoing Arabian plate?
4. More research is needed to test and refine models of Late Cretaceous subduction for Iran, the role of the Sanandaj-Sirjan Zone as the long lithospheric weakness required for subduction initiation, and what the Late Cretaceous ophiolites of Iran reveal about Late Cretaceous subduction initiation along the SW flank of Eurasia. These features suggest that Late Cretaceous subduction initiation in Iran may be an example of passive margin collapse to form a new subduction zone.

DISCLOSURE STATEMENT

The authors are not aware of any affiliations, memberships, funding, or financial holdings that might be perceived as affecting the objectivity of this review.

Annu. Rev. Earth Planet. Sci. 2021.49:9-36. Downloaded from www.annualreviews.org
Access provided by University of Texas - Dallas on 06/01/21. For personal use only.

Annu. Rev. Earth Planet. Sci. 2021.49:9-36. Downloaded from www.annualreviews.org
Access provided by University of Texas - Dallas on 06/01/21. For personal use only.

ACKNOWLEDGMENTS

Thanks to Surui Xie of the University of South Florida for making the GPS and Slab 2.0 map (**Figure 3**). We thank Emilie Bowman and Jordan Wang of the USGS for their comments on an early draft of this manuscript. This is UTD Geosciences contribution number 1375.

LITERATURE CITED

Abedi M, Bahroudi A. 2016. A geophysical potential field study to image the Makran subduction zone in SE Iran. *Tectonophysics* 688:119–34

Agard P, Omrani J, Jolivet L, Whitechurch H, Vrielynck B, et al. 2011. Zagros orogeny: a subduction-dominated process. *Geol. Mag.* 148(5–6):692–725

Ali SA, Buckman S, Aswad KJ, Jones BG, Ismail SA, Nutman AP. 2013. The tectonic evolution of a Neo-Tethyan (Eocene–Oligocene) island-arc (Walash and Naopurdan groups) in the Kurdistan region of the Northeast Iraqi Zagros Suture Zone. *Island Arc* 22:104–25

Alinaghi A, Koulakov I, Thybo H. 2007. Seismic tomographic imaging of *P*- and *S*-waves velocity perturbations in the upper mantle beneath Iran. *Geophys. J. Int.* 169:1089–102

Alothman AO, Fernandes RM, Bos MS, Schillak S, Elsaka B. 2016. Angular veocity of Arabian plate from multi-year analysis of GNSS data. *Arab. J. Geosci.* 9:529

Altamimi Z, Métivier L, Rebischung P, Rouby H, Collilieux X. 2017. ITRF2014 plate motion model. *Geophys. J. Int.* 209:1906–12

Arculus RJ, Gurnis M, Ishizuka O, Reagan MK, Pearce JA, Sutherland R. 2019. How to create new subduction zones: a global perspective. *Oceanography* 32:160–74

Asadi S, Moore F, Zarasvandi A. 2014. Discriminating productive and barren porphyry copper deposits in the southeastern part of the central Iranian volcano-plutonic belt, Kerman region, Iran: a review. *Earth-Sci. Rev.* 138:25–46

Ashrafi N, Jahangiri A, Hasebe N, Eby GN. 2018. Petrology, geochemistry and geodynamic setting of Eocene-Oligocene alkaline intrusions from the Alborz-Azerbaijan magmatic belt, NW Iran. *Geochemistry* 78:432–61

Asiabanha A, Foden J. 2012. Post-collisional transition from an extensional volcano-sedimentary basin to a continental arc in the Alborz Ranges, N-Iran. *Lithos* 148:98–111

Azizi H, Stern RJ. 2019. Jurassic igneous rocks of the central Sanadaj–Sirjan zone (Iran) mark a propagating continental rift, not a magmatic arc. *Terra Nova* 31:415–32

Babazadeh S, Ghorbani MR, Bröcker M, D'Antonio M, Cottle J, et al. 2017. Late Oligocene–Miocene mantle upwelling and interaction inferred from mantle signatures in gabbroic to granitic rocks from the Urumieh–Dokhtar arc, south Ardestan, Iran. *Int. Geol. Rev.* 59:1590–608

Babazadeh SA, De Wever P. 2004. Radiolarian Cretaceous age of Soulabest radiolarites in ophiolite suite of eastern Iran. *Bull. Soc. Geol. Fr.* 175:121–29

Bagheri S, Stampfli GM. 2008. The Anarak, Jandaq and Posht-e-Badam metamorphic complexes in central Iran: new geological data, relationships and tectonic implications. *Tectonophysics* 451:123–55

Ballato P, Uba CE, Landgraf A, Strecker MR, Sudo M, et al. 2011. Arabia-Eurasia continental collision: insights from late Tertiary foreland-basin evolution in the Alborz Mountains, northern Iran. *Geol. Soc. Am. Bull.* 123:106–31

Berberian M. 2014. *Earthquakes and Coseismic Surface Faulting on the Iranian Plateau*. Boston, MA: Elsevier

Berberian M, King GCP. 1981. Towards a paleogeography and tectonic evolution of Iran. *Can. J. Earth Sci.* 18:210–65

Bird P. 2003. An updated digital model of plate boundaries. *Geochem. Geophys. Geosyst.* 4(3):1027

Blewitt G, Hammond WC, Kreemer C. 2018. Harnessing the GPS data explosion for interdisciplinary science. *Eos* 99:1–2

Bowring SA, Grotzinger JP, Condon DJ, Ramezani J, Newall MJ, Allen PA. 2007. Geochronologic constraints on the chronostratigraphic framework of the Neoproterozoic Huqf Supergroup, Sultanate of Oman. *Am. J. Sci.* 307:1097–145

Bröcker M, Fotoohi Rad G, Burgess R, Theunissen S, Paderin I, et al. 2013. New age constraints for the geodynamic evolution of the Sistan Suture Zone, eastern Iran. *Lithos* 170–171:17–34

Burg JP. 2018. Geology of the onshore Makran accretionary wedge: synthesis and tectonic interpretation. *Earth-Sci. Rev.* 185:1210–31

Camp VE, Griffis RJ. 1982. Character, genesis and tectonic setting of igneous rocks in the Sistan suture zone, eastern Iran. *Lithos* 15:221–39

Castro A, Aghazadeh M, Badrzadeh Z, Chichorro M. 2013. Late Eocene–Oligocene post-collisional monzonitic intrusions from the Alborz magmatic belt, NW Iran. An example of monzonite magma generation from a metasomatized mantle source. *Lithos* 180:109–27

Christensen N, Mooney WD. 1995. Seismic velocity structure and composition of the continental crust: a global view. *J. Geophys. Res.* 100(B7):9761–88

Deevsalar R, Shinjo R, Ghaderi M, Murata M, Hoskin PWO, et al. 2017. Mesozoic–Cenozoic mafic magmatism in Sanandaj–Sirjan Zone, Zagros Orogen (Western Iran): geochemical and isotopic inferences from Middle Jurassic and Late Eocene gabbros. *Lithos* 284:588–607

Derakhshi M, Ghasemi H, Miao LC. 2017. Geochemistry and petrogenesis of Soltan Maidan basalts (E Alborz, Iran): implications for asthenosphere-lithosphere interaction and rifting along the N margin of Gondwana. *Geochemistry* 77:131–45

Dercourt J, Zonenshain L, Ricou L-E, Kazmin V, Le Pichon X, et al. 1986. Geological evolution of the Tethys belt from the Atlantic to the Pamirs since the Lias. *Tectonophysics* 123:241–315

Ding L, Spicer RA, Yang J, Xu Q, Cai F, et al. 2017. Quantifying the rise of the Himalaya orogen and implications for the South Asian monsoon. *Geology* 45:215–18

Ducea MN, Barton MD. 2007. Igniting flare-up events in Cordilleran arcs. *Geology* 35:1047–50

Etemad-Saeed N, Hosseini-Barzi M, Adabi MH, Miller NR, Sadeghi A, et al. 2015. Evidence for ca. 560 Ma Ediacaran glaciation in the Kahar Formation, central Alborz Mountains, northern Iran. *Gondwana Res.* 31:164–83

Fakhari MD, Axen GJ, Horton BK, Hassanzadeh J, Amini A. 2008. Revised age of proximal deposits in the Zagros foreland basin and implications for Cenozoic evolution of the High Zagros. *Tectonophysics* 451:170–85

Farhoudi G, Karig DE. 1977. Iran and Pakistan as an active arc system. *Geology* 5:664–68

Garfunkel Z. 2015. The relations between Gondwana and the adjacent peripheral Cadomian domain—constrains on the origin, history, and paleogeography of the peripheral domain. *Gondwana Res.* 28:1257–81

Garzanti E, Radeff G, Malusa MG. 2018. Slab breakoff: a critical appraisal of a geological theory as applied in space and time. *Earth-Sci. Rev.* 177:303–19

Ghorbani MR, Graham IT, Ghaderi M. 2014. Oligocene–Miocene geodynamic evolution of the central part of Urumieh-Dokhtar Arc of Iran. *Int. Geol. Rev.* 56:1039–50

Gordon RG. 1998. The plate tectonic approximation: plate nonrigidity, diffuse plate boundaries, and global plate reconstructions. *Annu. Rev. Earth Planet. Sci.* 26:615–42

Guilmette C, Smit M, van Hinsbergen DJJ, Gürer D, Corfu F, et al. 2018. Forced subdution initiation recorded in the sole and crust of the Semail Ophiolite of Oman. *Nat. Geosci.* 11:688–95

Hassanzadeh J, Wernicke BP. 2016. The Neotethyan Sanandaj-Sirjan zone of Iran as an archetype for passive margin-arc transitions. *Tectonics* 35:586–621

Hatzfeld D, Tatar M, Priestley K, Ghafory-Ashtiany M. 2003. Seismological constraints on the crustal structure beneath the Zagros Mountain belt (Iran). *Geophys. J. Int.* 155:403–10

Hayes GP, Moore GL, Portner DE, Hearne M, Flamme H, et al. 2018. Slab2, a comprehensive subduction zone geometry model. *Science* 262:58–61

Hessami K, Jamali F, Tabassi H. 2003. *Major active faults of Iran*. IIEES, Tehran International Institute of Earthquake Engineering and Seismology online database, Tehran, Iran. **http://www.iiees.ac.ir/en/**

Huber H. 1976. *Geological cross sections south-west Iran and northern Persian Gulf*, 1:500 000. National Iranian Oil Co.

Hunziker D, Burg J-P, Bouilhol P, von Quadt A. 2015. Jurassic rifting at the Eurasian Tethys margin: geochemical and geochronological constraints from granitoids of North Makran, southeastern Iran. *Tectonics* 34:571–93

Annu. Rev. Earth Planet. Sci. 2021.49:9-36. Downloaded from www.annualreviews.org
Access provided by University of Texas - Dallas on 06/01/21. For personal use only.

Jackson J, Priestly K, Allen M, Berberian M. 2002. Active tectonics of the south Caspian basin. *Geophys. J. Int.* 148:214–45

Jarvis A, Reuter HI, Nelson A, Guevara E. 2008. *Hole-filled SRTM for the globe Version 4*. CGIAR-CSI SRTM 90m Database, updated Nov. 2018. **http://srtm.csi.cgiar.org**

Jiménez-Munt I, Fernandez M, Saura E, Verges J, Garcia-Castellanos D. 2012. 3-D lithospheric structure and regional/residual Bouguer anomalies in the Arabia–Eurasian collision (Iran). *Geophys. J. Int.* 190:1311–24

Kaban MK, El Khrepy S, Al-Arifi N, Tesauro M, Stolk W. 2016. Three-dimensional density model of the upper mantle in the Middle East: interaction of diverse tectonic processes. *J. Geophys. Res. Solid Earth* 121:5349–64

Khalatbari-Jafari M, Juteau T, Cotten J. 2006. Petrological and geochemical study of the Late Cretaceous ophiolite of Khoy (NW Iran), and related geological formations. *J. Asian Earth Sci.* 27:465–502

Kheirkhah M, Neill I, Allen MB. 2015. Petrogenesis of OIB-like basaltic volcanic rocks in a continental collision zone: Late Cenozoic magmatism of Eastern Iran. *J. Asian Earth Sci.* 106:19–33

Khorrami F, Vernant P, Masson F, Nilfouroushan F, Mousavi Z, et al. 2019. An up-to-date crustal deformation map of Iran using integrated campaign-mode and permanent GPS velocities. *Geophys. J. Int.* 21:832–43

Koshnaw RI, Stockli DF, Schlunegger F. 2018. Timing of the Arabia-Eurasia continental collision—evidence from detrital zircon U-Pb geochronology of the Red Bed Series strata of the northwest Zagros hinterland, Kurdistan region of Iraq. *Geology* 47:47–50

Mahmoodabadi M, Yaminifard F, Tatar M, Kaviani A, Motaghi K. 2019. Upper-mantle velocity structure beneath the Zagros collision zone, central Iran and Alborz from nonlinear teleseismic tomography. *Geophys. J. Int.* 218:414–28

Malekpour-Alamdari A, Axen G, Heizler M, Hassanzadeh J. 2017. Large-magnitude continental extension in the northeastern Iranian Plateau: insight from K-feldspar $^{40}Ar/^{39}Ar$ thermochronology from the Shotor Kuh–Biarjmand metamorphic core complex. *Geosphere* 13:1207–33

Martinez F, Goodliffe AM, Taylor B. 2001. Metamorphic core complex formation by density inversion and lower-crust extrusion. *Nature* 411:930–34

McCall GJH. 1985. *Explanatory text of the Minab Quadrangle*, *Map*, 1:250,000, No. J13. Geological Survey of Iran, Tehran.

McCall GJH. 2002. A summary of the geology of the Iranian Makran. *Geol. Soc. Lond. Spec. Publ.* 195:147–204

McQuarrie N, Stock JM, Verdel C, Wernicke BP. 2003. Cenozoic evolution of Neotethys and implications for the causes of plate motions. *Geophys. Res. Lett.* 30:2036

Mirnejad H, Lalonde AE, Obeid M, Hassanzadeh J. 2013. Geochemistry and petrogenesis of Mashhad granitoids: an insight into the geodynamic history of the Paleo-Tethys in northeast of Iran. *Lithos* 170:105–16

Mirnejad H, Raeisi D, McFarlane C, Sheibi M. 2018. Tafresh intrusive rocks within the Urumieh-Dokhtar Magmatic Arc: appraisal of Neo-Tethys subduction. *Geol. J.* 54:1745–55

Monsef I, Monsef R, Mata J, Zhang Z, Pirouz M, et al. 2018. Evidence for an early-MORB to fore-arc evolution within the Zagros suture zone: constraints from zircon U-Pb geochronology and geochemistry of the Neyriz ophiolite (South Iran). *Gondwana Res.* 62:287–305

Mooney WD. 2015. Crust and lithospheric structure—global crustal structure. In *Treatise on Geophysics*, Vol. 1: *Seismology and Structure of the Earth*, ed. B Romanowicz, A Dziewonski, pp. 339–90. Amsterdam: Elsevier. 2nd ed.

Moritz R, Ghazban F, Singer BS. 2006. Eocene gold ore formation at Muteh, Sanandaj-Sirjan tectonic zone, western Iran: a result of late-stage extension and exhumation of metamorphic basement rocks within the Zagros orogen. *Econ. Geol.* 101:1497–524

Mouthereau F, Lacombe O, Verges J. 2012. Building the Zagros collisional orogen: timing, strain distribution and the dynamics of Arabia/Eurasia plate convergence. *Tectonophysics* 532:27–60

Neill I, Meliksetian K, Allen MB, Navasardyan G, Kuiper K. 2015. Petrogenesis of mafic collision zone magmatism: the Armenian sector of the Turkish-Iranian Plateau. *Chem. Geol.* 403:24–41

Nemati M. 2019. Seismotectonic and seismicity of Makran, a bimodal subduction zone, SE Iran. *J. Asian Earth Sci.* 169:139–61

Neuendorf KKE, Mehl JP, Jackson JA. 2011. *Glossary of Geology*, p. 457. London: Springer. 5th ed.

Annu. Rev. Earth Planet. Sci. 2021.49:9-36. Downloaded from www.annualreviews.org
Access provided by University of Texas - Dallas on 06/01/21. For personal use only.

Pang KN, Chung SL, Zarrinkoub MH, Chiu HY, Li XH. 2014. On the magmatic record of the Makran arc, southeastern Iran: insights from zircon U-Pb geochronology and bulk-rock geochemistry. *Geochem. Geophys. Geosyst.* 15:2151–69

Pang KN, Chung SL, Zarrinkoub MH, Khatib MM, Mohammadi SS, et al. 2013. Eocene–Oligocene post-collisional magmatism in the Lut–Sistan region, eastern Iran: magma genesis and tectonic implications. *Lithos* 180:234–51

Pang KN, Chung SL, Zarrinkoub MH, Li XH, Lee HY, et al. 2016. New age and geochemical constraints on the origin of Quaternary adakite-like lavas in the Arabia Eurasia collision zone. *Lithos* 264:348–59

Pang KN, Chung SL, Zarrinkoub MH, Mohammadi SS, Yang HM, et al. 2012. Age, geochemical characteristics and petrogenesis of Late Cenozoic intraplate alkali basalts in the Lut-Sistan region, eastern Iran. *Chem. Geol.* 306:40–53

Pang KN, Chung SL, Zarrinkoub MH, Wang F, Kamenetsky VS, Lee HY. 2015. Quaternary high-Mg ultrapotassic rocks from the Qal'eh Hasan Ali maars, southeastern Iran: petrogenesis and geodynamic implications. *Contrib. Mineral. Petrol.* 170:27

Pirouz M, Avouac J-P, Hassanzadeh J, Kirschvink JL, Bahroudi A. 2017. Early Neogene foreland of the Zagros, implications for the initial closure of the Neo-Tethys and kinematics of crustal shortening. *Earth Planet. Sci. Lett.* 477:168–82

Pirouz M, Simpson G, Bahroudi A, Azhdari A. 2011. Neogene sediments and modern depositional environments of the Zagros foreland basin system. *Geol. Mag.* 148:838–53

Prodehl C, Mooney WD. 2012. *Exploring the Earth's Crust: History and Results of Controlled-Source Seismology*. Boulder, CO: Geol. Soc. Am.

Ramezani J, Tucker RD. 2003. The Saghand region, Central Iran: U-Pb geochronology, petrogenesis and implications for Gondwana tectonics. *Am. J. Sci.* 303:622–65

Reilinger R, McClusky S. 2011. Nubia-Arabia-Eurasia plate motions and the dynamics of Mediterranean and Middle East tectonics. *Geophys. J. Int.* 186:971–79

Reymer A, Schubert G. 1984. Phanerozoic addition rates to the continental crust and crustal growth. *Tectonics* 3:63–77

Saura E, Garcia-Castellanos D, Casciello E, Parravano V, Urruela A, Verges J. 2015. Modeling the flexural evolution of the Amiran and Mesopotamian foreland basins of NW Zagros (Iran–Iraq). *Tectonics* 34:377–95

Sepidbar F, Lucci F, Biabangard H, Khhedr MZ, Jiantang P. 2020. Geochemistry and tectonic significance of the Fannuj-Maskutan SSZ-type ophiioliite (Inner Makran, SE Iran). *Int. Geol. Rev.* 62:2077–104

Sepidbar F, Mirnejad H, Ma C, Shafaii Moghadam H. 2018. Identification of Eocene-Oligocene magmatic pulses associated with flare-up in east Iran: timing and sources. *Gondwana Res.* 57:141–56

Seyed-Emami K. 2003. Triassic in Iran. *Facies* 48:91–106

Shafaii Moghadam H, Corfu F, Chiaradia M, Stern RJ, Ghorbani G, Rossetti F. 2014. Sabzevar Ophiolite, NE Iran: progress from embryonic oceanic lithosphere into magmatic arc constrained by new isotopic and geochemical data. *Lithos* 210–211:224–41

Shafaii Moghadam H, Griffin WL, Kirchenbaur M, Garbe-Schnoberg D, Khedr MZ, et al. 2018. Roll-back, extension and mantle upwelling triggered Eocene potassic magmatism in NW Iran. *J. Petrol.* 59:1417–65

Shafaii Moghadam H, Griffin WL, Li X-H, Stern RJ, Karsli O, et al. 2017. Crustal evolution of NW Iran: Cadomian arcs, Archean fragments and the Cenozoic magmatic flare-up. *J. Petrol.* 58:2143–90

Shafaii Moghadam H, Li QL, Griffin WL, Stern RJ, Ishizuka O, et al. 2020a. Repeated magmatic buildup and deep "hot zones" in continental evolution: the Cadomian crust of Iran. *Earth Planet. Sci. Lett.* 531:115989

Shafaii Moghadam H, Li QL, Stern RJ, Chiaradia M, Karsli O, Rahimzadeh B. 2020b. The Paleogene ophiolite conundrum of the Iran–Iraq border. *J. Geol. Soc. Lond.* 177:955–64

Shafaii Moghadam H, Li X-H, Ling X-X, Santos JF, Stern RJ, et al. 2015a. Eocene Kashmar granitoids (NE Iran): petrogenetic constraints from U-Pb zircon geochronology and isotope geochemistry. *Lithos* 216–217:118–35

Shafaii Moghadam H, Li X-H, Ling X-X, Stern RJ, Santos JF, et al. 2015b. Petrogenesis and tectonic implications of Late Carboniferous A-type granites and gabbronorites in NW Iran: geochronological and geochemical constraints. *Lithos* 212–215:266–79

Annu. Rev. Earth Planet. Sci. 2021.49:9-36. Downloaded from www.annualreviews.org
Access provided by University of Texas - Dallas on 06/01/21. For personal use only.

Shafaii Moghadam H, Stern RJ. 2011. Geodynamic evolution of Upper Cretaceous Zagros ophiolites: formation of oceanic lithosphere above a nascent subduction zone. *Geol. Mag.* 148:762–801
Shafaii Moghadam H, Stern RJ. 2014. Ophiolites of Iran: keys to understanding the tectonic evolution of SW Asia: (I) Paleozoic ophiolites. *J. Asian Earth Sci.* 91:19–38
Shafaii Moghadam H, Stern RJ. 2015. Ophiolites of Iran: keys to understanding the tectonic evolution of SW Asia: (II) Mesozoic ophiolites. *J. Asian Earth Sci.* 100:31–59
Smith AG. 2012. A review of Ediacaran to Early Cambrian ('Infra-Cambrian') evaporites and associated sediments of the Middle East. *J. Geol. Soc. Lond.* 366:229–50
Stampfli GM. 2000. Tethyan oceans. *Geol. Soc. Lond. Spec. Publ.* 173:1–23
Stampfli GM, Borel GD. 2002. A plate tectonic model for the Paleozoic and Mesozoic constrained by dynamic plate boundaries and restored synthetic oceanic isochrons. *Earth Planet. Sci. Lett.* 196:17–33
Stampfli G, Borel GD, Cavazza W, Mosar J, Ziegler P. 2001. Palaeotectonic and palaeogeographic evolution of the western Tethys and PeriTethyan domain (IGCP Project 369). *Episodes* 24:222–28
Stern RJ. 2002. Subduction zones. *Rev. Geophys.* 40:1012
Stern RJ, Gerya T. 2018. Subduction initiation in nature and models: a review. *Tectonophysics* 746:173–98
Stern RJ, Johnson P. 2010. Continental lithosphere of the Arabian plate: a geologic, petrologic, and geophysical synthesis. *Earth–Sci. Rev.* 101:29–67
Stern RJ, Johnson PR. 2019. Constraining the opening of the Red Sea: evidence from the Neoproterozoic margins and Cenozoic magmatism for a volcanic rifted margin. In *Geological Setting of the Red Sea*, ed. NMA Rasul, ICF Stewart, pp. 53–80. Cham, Switz.: Springer
Stocklin J. 1968. Structural history and tectonics of Iran: a review. *AAPG Bull.* 52:1229–58
Tirrul R, Bell IR, Griffis RJ, Camp VE. 1983. The Sistan suture zone of eastern Iran. *Geol. Soc. Am. Bull.* 94:134–50
van Hinsbergen DJ, Steinberger B, Doubrovine PV, Gassmöller R. 2011. Acceleration and deceleration of India-Asia convergence since the Cretaceous: roles of mantle plumes and continental collision. *J. Geophys. Res.* 116(B6):B06101
Verdel C, Wernicke BP, Hassanzadeh J, Guest B. 2011. A Paleogene extensional arc flare-up in Iran. *Tectonics* 30:TC3008
Verdel C, Wernicke BP, Ramezani J, Hassanzadeh J, Renne PR, Spell TL. 2007. Geology and thermochronology of Tertiary Cordilleran-style metamorphic core complexes in the Saghand region of central Iran. *Geol. Soc. Am. Bull.* 119:961–77
Zare M, Amini H, Yazdi P, Sesetyan K, Demircioglu MB, et al. 2014. Recent developments of the Middle East catalog. *J. Seismol.* 18:749–72

Annu. Rev. Earth Planet. Sci. 2021.49:9-36. Downloaded from www.annualreviews.org
Access provided by University of Texas - Dallas on 06/01/21. For personal use only.

Annual Review
of Earth and
Planetary Sciences
Volume 49, 2021

Contents

Annu. Rev. Earth Planet. Sci. 2021.49:9-36. Downloaded from www.annualreviews.org
Access provided by University of Texas - Dallas on 06/01/21. For personal use only.

Errata

An online log of corrections to *Annual Review of Earth and Planetary Sciences* articles may be found at http://www.annualreviews.org/errata/earth

Annu. Rev. Earth Planet. Sci. 2021.49:9-36. Downloaded from www.annualreviews.org
Access provided by University of Texas - Dallas on 06/01/21. For personal use only.